Title of Thesis

The Neural Substrates of Motion Inhibitory Control During Go/No-Go Response Inhibition Task

September, 2024

ZHANG NAN

Graduate School of Interdisciplinary

Science and Engineering in Health Systems

（Doctor’s Course）

OKAYAMA UNIVERSITY

Abstract

Response inhibition refers to an individual's ability to suppress automatic or habitual reactions when faced with inappropriate or irrelevant stimuli. This process is crucial in daily life as it involves multiple aspects, such as decision-making, attention control, and impulse management. The Go/No-Go task is a classic paradigm for studying response inhibition, requiring individuals to respond to specific stimuli (Go signals) while inhibiting responses to other stimuli (No-Go signals), thereby assessing their capacity for response inhibition. Although previous studies have shown that different Go/No-Go ratios affect response inhibition, these studies mainly focus on fixed ratio settings. A systematic exploration of the mechanisms of response inhibition under various ratio and interval combinations has not yet been conducted.

This study aims to investigate the effects of different Go/No-Go ratios on response inhibition. Through behavioral experiments, event-related potential (ERP) experiments, and complex network analysis, we systematically studied the impact of ratio changes in the Go/No-Go task on the behavioral and neural mechanisms of response inhibition. Our study contributes to a deeper understanding of how varying task conditions affect cognitive control processes, which is essential for developing effective interventions for disorders involving impaired inhibition, such as ADHD and OCD.

In the behavioral experiment, we set different Go/No-Go ratios (100%:0%, 75%:25%, 50%:50%, 25%:75%) and three different intervals (100 ms, 300 ms, 500 ms), recording

participants' reaction times in the Go task. The results showed that as the proportion of Go tasks decreased, the reaction time significantly increased. This suggests that a lower frequency of Go signals makes it harder for participants to maintain a quick response, likely due to the increased cognitive load required to frequently inhibit responses. The interval time had no significant effect on reaction time, indicating that the ratio of Go/No-Go signals is a more critical factor in determining reaction speed than the timing between stimuli. However, reaction times tended to stabilize after 300 ms, which may reflect an optimal processing window for participants to prepare their responses.

In the ERP experiment, we focused on the No-Go P3 component, a well-known marker of cognitive control processes related to inhibition. We found that as the proportion of No-Go tasks increased, the amplitude and latency of the No-Go P3 significantly decreased. This indicates a reduction in inhibition capacity and processing speed, suggesting that participants may become less efficient at processing and responding to No-Go signals when they occur more frequently. This finding aligns with previous research suggesting that increased demands on inhibitory control can lead to neural adaptations that impact overall cognitive performance.

Through complex network analysis, we further analyzed the dynamic characteristics of EEG data. The results showed that as the proportion of Go tasks decreased, the characteristic path length of brain networks shortened, local efficiency increased, global efficiency decreased, and the clustering coefficient increased. These changes indicate that under

conditions with more No-Go tasks, the brain's information processing pathways and speed decreased. Specifically, the increased local efficiency and clustering coefficient suggest that the brain might rely more on localized processing and less on global integration when faced with frequent inhibitory demands. Additionally, the betweenness centrality of the central region increased, highlighting its importance in the response inhibition network. This increase in centrality indicates that the central region becomes a more crucial hub for coordinating the network's overall activity, reflecting its role in managing complex inhibitory processes.

The findings from our behavioral and ERP experiments, combined with the insights gained from complex network analysis, provide a comprehensive picture of how different Go/No-Go ratios influence response inhibition. This study highlights the importance of considering task parameters in cognitive research and suggests that varying these parameters can significantly alter both behavioral outcomes and neural processes. Understanding these effects is essential for designing more effective cognitive training programs and therapeutic interventions for individuals with inhibitory control deficits.

In our behavioral experiment, participants were presented with visual stimuli of green triangles pointing in four directions. They were instructed to quickly move the joystick in the same direction as the cue when it matched the target direction and to inhibit their response when it pointed in a different direction. This setup allowed us to systematically vary the Go/No-Go ratios and intervals to assess their impact on reaction times. Our findings revealed significant differences between the different ratios, with reaction times increasing as the

number of Go tasks decreased. This suggests that the frequency of Go signals plays a crucial role in maintaining quick response times, likely due to the increased cognitive load required to inhibit responses more frequently.

In the ERP experiment, we obtained average data from nine electrodes in the central region to investigate the neural mechanisms of response inhibition. The results showed that as the proportion of No-Go tasks increased, the amplitude and latency of the No-Go P3 component significantly decreased. This reduction in amplitude and latency suggests a decrease in both inhibition capacity and information processing speed. These findings are consistent with the hypothesis that increased demands on inhibitory control lead to neural adaptations that impact cognitive performance. The No-Go P3 component is particularly sensitive to changes in task demands, making it a valuable marker for studying the neural underpinnings of inhibitory control.

In the complex network analysis, we analyzed the functional connectivity of EEG data to reveal the dynamic characteristics of brain information processing under different ratio conditions. At the global level, as the proportion of Go tasks decreased, global efficiency, local efficiency, and the clustering coefficient showed decreasing trends, while the characteristic path length showed an increasing trend. These results indicate that under conditions with more No-Go tasks, the brain's information processing pathways and speed decreased. Specifically, the increased local efficiency and clustering coefficient suggest that the brain relies more on localized processing when faced with frequent inhibitory demands.

ABSTRACT

The decrease in betweenness centrality of the central region highlights its importance as a hub for coordinating the network's activity during complex inhibitory processes.

Overall, this study reveals the significant impact of different Go/No-Go ratios on the behavioral and neural mechanisms of response inhibition, providing a new perspective for understanding the dynamic characteristics of response inhibition. These findings will contribute to the development of more refined experimental designs and analytical methods in future neuroscience research. By highlighting the importance of task parameters, this study underscores the need for careful consideration of these factors in both experimental and clinical settings. This enhanced understanding of response inhibition mechanisms can inform the development of targeted interventions for disorders involving impaired inhibitory control, ultimately improving cognitive health and performance.

Keyword: Go/No-Go; response inhibition; ERPs; NoGo-P3; ratio; complex network analysis

Content

1. Introduction

1.1. Response inhibition

Response inhibition is a crucial component of executive control, referring to the ability to suppress behaviors that are no longer needed or are inappropriate in a constantly changing environment. It forms the basis of a series of adaptive functions [1], [2]. This ability is particularly important in dynamic environments, with ample evidence linking impaired inhibition control to various mental disorders. The neural mechanisms of response inhibition mainly involve the prefrontal cortex—especially the right prefrontal cortex—the anterior cingulate gyrus, and the basal ganglia [3], [4]. These brain regions work together to monitor and regulate behavior, ensuring individuals can effectively suppress inappropriate responses. Response inhibition is considered a vital function for achieving goal-directed behavior, aiding individuals in maintaining focus and control when faced with interference or temptation [5].

In daily life, response inhibition is omnipresent. We can stop speaking, walking, or typing at any moment to adapt to changes in internal states or the environment [6]. For instance, while driving a car, we must constantly pay attention to safety cues in our surroundings and promptly stop when we see a red light or encounter sudden hazards, such as jaywalking pedestrians, to ensure the safety of ourselves and others. In social situations, we need to curb impulsive behaviors to maintain politeness and appropriate social conduct. In learning and work environments, we must suppress responses to distractions to maintain focus and efficiency [7], [8]. The ability of response inhibition enables us to flexibly adapt to various environmental changes and task demands, thus facilitating goal-directed behavior.

Abnormalities in response inhibition are closely associated with various mental and neurological disorders. For example, patients with Parkinson's disease (PD) often exhibit impulse control disorders (ICD) and impaired selective response inhibition. In a functional magnetic resonance imaging (fMRI) study, PD patients showed reduced functionality in the pre-supplementary motor area, medial prefrontal cortex, and orbitofrontal cortex during tasks [9], [10], [11]. Dysfunction in the fronto-striatal and fronto-striato-thalamo-cortical circuits may reflect impaired metacognitive executive functions (such as response inhibition, action monitoring, and error awareness), leading to compulsive repetitive behaviors. Attention Deficit Hyperactivity Disorder (ADHD) patients also demonstrate response inhibition issues. These problems are not limited to children but also extend to adults. ADHD patients exhibit deficits in delayed response, interruption of ongoing responses following feedback about performance, and inhibition of responses to distractors while performing tasks that require self-regulation and goal-directed actions. Literature consistently suggests that inhibitory deficits resulting from ADHD appear to be specific to the disorder and not caused by other commonly co-occurring conditions (such as mood, anxiety, and learning disorders) [12], [13], [14]. Impulsive behavior is also closely related to response inhibition, particularly in the identification of borderline personality disorder and antisocial personality disorder. Poor impulse control is significantly correlated with suicide, violence, and aggressive behaviors, making it an increasingly important aspect of risk assessment in various clinical scenarios [15], [16]. Investigating response inhibition not only contributes to understanding how humans adapt to their environment through flexible behavior but also enhances comprehension of mental and neurological disorders, holding significant implications for both basic theory and

clinical guidance.

1.2. GO/No-Go Task

Go/No-Go tasks are classic neuropsychological experiments designed to measure an individual's ability to respond to external stimuli and inhibit responses [17], [18]. These tasks typically involve two types of stimuli: Go stimuli and No-Go stimuli. Participants are required to respond quickly to Go stimuli but must inhibit their response to No-Go stimuli [15]. This design allows researchers to examine inhibitory response capabilities while minimizing interference from other cognitive and behavioral processes. In the study of response inhibition, Go/No-Go tasks offer numerous advantages, such as a simple design, ease of implementation, and the ability to directly measure inhibition by recording successful inhibition of responses to No-Go stimuli [19]. Additionally, Go/No-Go tasks combine two types of experimental paradigms—choice reaction tasks and simple reaction time tasks—enabling the simultaneous assessment of both response selection and response inhibition.

Inhibitory control is a core function that enables us to resist interference and stop ongoing actions [20]. A study involving 20 eight-year-old children and 17 adults performing Go/No-Go tasks found that response inhibition exists in both children and adults, while interference inhibition is present only in adults, indicating different maturation processes [21]. High-density EEG recordings revealed that the N2 component is associated with response inhibition, with a greater negative amplitude observed in No-Go trials. Go/No-Go tasks and Stop Signal Tasks (SST) demonstrate different inhibition mechanisms and neural dynamics, suggesting they should not be used interchangeably [22]. Functional MRI (fMRI) studies using Go/No-

Go tasks have revealed different brain regions activated by various versions of inhibition tasks. Some studies have also found significant correlations between response inhibition and certain traits of psychopathy [23], [24]. Automatic response inhibition relies on consistent stimulus-stop associations and improves with practice. Overall, Go/No-Go tasks are powerful tools for studying response inhibition and are widely used to explore the relationship between inhibition ability and neural activity, as well as their roles in cognitive functions and diseases [25], [26]. Despite some design limitations, such as lack of ecological validity and ceiling effects, researchers are advancing the understanding of the neural mechanisms and behavioral manifestations of response inhibition by improving task design and combining it with other paradigms.

1.3. EEG

1.3.1. EEG signal

The electroencephalogram (EEG) was first described in 1875 by Liverpool physician Richard Caton, who observed electrical oscillations on the exposed cortical surface of animals [27], [28]. In 1929, Jena psychiatrist Hans Berger began a series of reports that are widely regarded as the first systematic descriptions of human EEGs. Over the next 50 years, significant improvements were made in the equipment used to transmit, amplify, and display EEGs. In the past 20 years, there have been advances in understanding the relationship between brain electrophysiology and the origins of EEG waveforms. EEG activity exhibits complex behavior with strong nonlinear and dynamic characteristics. Communication between brain cells occurs through electrical pulses [29], [30]. EEG is measured by placing electrodes on the subject's scalp. Inhibitory and excitatory postsynaptic potentials of cortical

nerve cells generate EEG signals. These postsynaptic potentials aggregate in the cortex and extend to the scalp surface, where they are recorded as EEGs [31]. The typical amplitude of EEG signals measured from the scalp ranges from approximately 10 μV to 100 μV, with a frequency range of 1 Hz to about 100 Hz.

EEG can record brain electrical activity in real time, providing researchers with immediate brain wave data to help understand the brain's responses to different psychological states and cognitive tasks [32]. Its millisecond-level time resolution allows it to capture rapid changes in brain activity, which is crucial for studying the dynamic changes in fast cognitive processes such as attention, perception, and memory. In psychological experiments, EEG can be used to design and validate various experimental paradigms and tasks [33]. For example, by analyzing brain activity under different experimental conditions, researchers can optimize experimental design and improve both internal and external validity. Additionally, EEG is a non-invasive method of measuring brain electrical activity that does not cause physiological harm or discomfort to participants. This makes it readily acceptable and applicable in psychological experiments, especially for children and other sensitive groups. By analyzing brain waves, researchers can explore the neural basis of different cognitive processes, such as attention, memory, learning, and decision-making. EEG can also be used to study the neural mechanisms of emotions and affect. For example, by measuring brain wave activity under different emotional states, researchers can reveal the neural basis of emotion regulation and gain insights into the mechanisms of emotional disorders.

EEG is also a non-invasive technique used to diagnose brain-related diseases and symptoms. It aids in diagnosing many neurological disorders, such as epilepsy, tumors, cerebrovascular lesions, depression, and trauma-related issues [34], [35]. Different brain activities produce distinct EEG patterns. By comparing EEG signals from healthy individuals and patients, researchers can identify brain electrical characteristics associated with specific psychopathological states. For example, epileptic patients' EEG signals exhibit characteristic epileptic discharge patterns, and alpha wave activity may be reduced in patients with depression. Moreover, EEG plays an irreplaceable role in sleep research. By recording brain wave activity during different sleep stages, researchers can gain in-depth insights into sleep structure and function and study the causes and treatments of sleep disorders.

EEG can be combined with other neuroimaging techniques (such as fMRI and MEG) to provide more comprehensive information about brain function. Multimodal research can integrate the strengths of different techniques to reveal the spatiotemporal dynamics of complex cognitive processes. EEG also has significant applications in brain-computer interface (BCI) research. By analyzing EEG signals, researchers can develop technologies that translate brain activity into control signals for devices, enabling individuals with disabilities to express their intent and control devices [36]. In the field of psychology, EEG holds significant importance. By providing real-time, non-invasive recordings of brain electrical activity, it offers high temporal resolution brain function data. EEG plays a crucial role in various research areas, such as cognition, emotion, sleep, mental disorders, and brain-computer interfaces, helping researchers uncover the neural mechanisms of brain

functions and advancing psychological theory and practice.

1.3.2. EEG features

Brain waves have unique characteristics that constantly change in their time and spatial distribution. Thus, the potential (amplitude), time (period), and phase of brain waves form the basic features of an EEG [37]. The period of brain waves is slightly different from the period of sine waves in physics. It refers to the time from the trough (or peak) of one wave to the trough (or peak) of the next wave, measured in milliseconds. The number of periods that occur per second is called the frequency, expressed in Hertz (Hz). On an EEG, besides waveforms similar to sine waves, composite waves consisting of overlapping brain waves with different periods can also be observed [38].

The amplitude of brain waves is usually measured by drawing a vertical line from the peak to intersect with the line connecting the troughs of the preceding and succeeding waves. The distance from this intersection point to the peak is called the amplitude and is expressed in microvolts (μV). This measurement method is used because the EEG baseline is often unstable. The amplitude of brain waves is primarily determined by the intensity of electrical activity occurring within the brain and the choice of reference electrodes. Brain waves are generally classified into four types based on amplitude: low amplitude (below 25 μV), medium amplitude (25-75 μV), high amplitude (75-150 μV), and extremely high amplitude (above 150 μV) [39]. Changes in brain wave amplitude can be broadly divided into three types: very rapid sudden changes, such as epileptic waves; changes over a short period (tens of milliseconds to a few minutes) due to stimuli like eye-opening in a closed-eye state, external stimuli, and

mental activities; and slow amplitude changes over a period of days to several years due to development or aging [40], [41], [42].

The phase of brain waves is also referred to as the polarity of brain waves. Usually, a wave with a peak above the baseline is called a positive wave, and a wave with a peak below the baseline is called a negative wave [43]. It should be noted that in EEG recordings, negative potentials are typically recorded above the baseline, while positive potentials are recorded below the baseline. Based on the phase, brain waves can be monophasic, biphasic, or multiphasic. When observing and comparing brain waves at two locations simultaneously, the phase relationship between them is an important indicator. If the brain waves at two locations have the same period and phase at the same time point, they are called in-phase. If the brain waves at two locations deflect in opposite directions from the baseline at the same time, they are called out-of-phase [44]. In healthy individuals, α waves in symmetrical regions of the brain are generally in-phase, especially between the left and right occipital regions. However, phase differences can exist between the left and right parietal regions, and phase inversion can be seen between the occipital and frontal regions. The phase relationship of brain waves is significant for the localization of brain function impairments.

In human EEGs, brain wave frequencies typically range from 0.5 to 30 Hz and are usually classified based on frequency to represent various components. Below are the international classification standards. Generally, θ waves and δ waves, which are slower than α waves, are collectively referred to as slow waves, while β waves and γ waves, which are faster than

α waves, are collectively called fast waves [45]. Additionally, brain waves that appear under specific conditions, such as pathological conditions, are named according to their waveform characteristics and significance, including spike waves, spike-slow composite waves, vertex waves, and triphasic waves.

The average amplitude of α waves in healthy adults is 30-50 μV, with these waves mainly distributed in the parietal-occipital regions and generally resembling sine waves. α waves are a primary component of the EEG in most healthy adults, appearing most frequently and with the highest amplitude in a relaxed awake state with closed eyes. α waves completely disappear during sleep. When awake, their amplitude decreases upon eye-opening or when attention is focused and is replaced by higher frequency β waves [46]. α waves change with brain development and age. In children, the number and frequency of α waves gradually increase with brain development, stabilize in adulthood, and decrease with age. Therefore, the frequency, amplitude, and spatial distribution of α waves are important indicators of the brain's functional state.

The frequency range of β waves is 14-30 Hz, with amplitudes generally ranging from 5 to 30 μV. These waves are distributed throughout the brain, primarily in the frontal and temporal regions. Approximately 6% of the EEGs of healthy adults are dominated by β wave activity [47]. β waves may be related to factors such as gender, psychology, personality, and age. Generally, β waves are more common in females than in males and more common in the elderly than in younger adults. β waves often increase in number and amplitude during

emotional instability or with the use of sedative-hypnotic drugs. β waves can be further divided into β1 and β2. β1 waves have a frequency of approximately 13-20 Hz and, like α waves, are influenced by psychological activities. β2 waves have a frequency of approximately 20-30 Hz and appear during intense activity or tension in the central nervous system.

θ waves have a frequency of 4-7 Hz and an amplitude of 10-40 μV. From childhood to adulthood, the number of θ waves gradually decreases, their frequency increases, and their amplitude decreases [48]. In healthy adult EEGs, θ waves appear sporadically and infrequently. In children, θ waves mainly occur in the parietal and temporal regions, while in adults, they can appear during emotional suppression, particularly in states of disappointment and frustration, for up to nearly 20 seconds. The number of θ waves increases with fatigue or after falling asleep. θ waves are also common in old age and in pathological conditions.

δ waves appear during deep sleep, in infants, and in patients with severe organic brain diseases. These δ waves can also be recorded in the brains of experimental animals after subcortical transections, which functionally separate the cerebral cortex from the reticular activating system [47]. Therefore, δ waves occur only within the cortex and are not controlled by the brain's lower-level nerve structures.

1.3.3. ERP techniques

Event-related potentials (ERPs) are a special type of brain-evoked potential induced by deliberately providing stimuli with specific psychological significance and using multiple or

varied stimuli to elicit brain potentials. They reflect neuro-electrophysiological changes in the brain during cognitive processes and are also known as cognitive potentials. This term refers to the brain potentials recorded from the scalp when individuals engage in cognitive processing of a particular task [49].

Objectively evaluating advanced psychological activities of the brain, such as cognitive processes, is challenging because it is difficult to attribute consciousness or thought solely to changes in specific parts of the brain, its tissues, cells, or neurotransmitters [50]. Using only concrete and microscopic natural science methods, such as neuro-molecular biology and neuro-biochemistry, is insufficient to address specific psychological activities. In the 1960s, Sutton introduced the concept of event-related potentials. By using an averaging technique to record brain-evoked potentials from the scalp, this method reflects neuro-electrophysiological changes in the brain during cognitive processes. Due to the close relationship between ERPs and cognitive processes, they are considered a "window" into observing psychological activities. The development of neuro-electrophysiological techniques has provided new methods and approaches for studying the cognitive processes of the brain.

ERPs differ from ordinary evoked potentials in that subjects are generally required to be awake; the stimuli are not single, repetitive flashes or short sounds, but at least two or more types of stimuli arranged in a sequence (the stimuli can be visual, auditory, numerical, linguistic, or images). ERPs consist of exogenous components, which are influenced by the

physical characteristics of the stimuli, and endogenous components, which are unaffected by these physical characteristics. The endogenous components are closely related to cognitive processes [51], [52]. Endogenous ERPs differ significantly from exogenous stimulus-related potentials. ERPs are associated with psychological activities such as recognition, comparison, judgment, memory, and decision-making, reflecting different aspects of cognitive processes, making them a "window" into understanding brain cognitive functions. Classic ERP components include P1, N1, P2, N2, and P3 (P300). Among these, P1, N1, and P2 are exogenous (physiological) components influenced by the physical characteristics of stimuli, while N2 and P3 are endogenous (psychological) components unaffected by the physical characteristics of stimuli and are related to the subject's mental state and attention [53]. The concept of ERPs has expanded to include additional components such as N4 (N400), Mismatch Negativity (MMN), and Contingent Negative Variation (CNV).

1.4. Analysis methods of EEG

1.4.1. Conventional analysis methods

EEG signals can be analyzed using various techniques to understand their characteristics and underlying brain activities. The main analysis methods include time-domain analysis, frequency-domain analysis, and time-frequency analysis.

Time-domain analysis involves examining how EEG signals change over time. This method focuses on the amplitude and shape of EEG waves recorded from the scalp [54]. The relevant methods include: 1. Waveform analysis: Assessing the shape of waves such as alpha waves, beta waves, theta waves, and delta waves, which correspond to different brain states and

activities. 2. Amplitude: Measuring the height of waves (typically in microvolts, μV), indicating the intensity of brain activity. 3. Latency: Determining the time interval between stimuli and the corresponding EEG response. 4. ERPs: Analyzing specific patterns time-locked to stimuli or events, providing insights into cognitive processes.

Frequency-domain analysis uses techniques like the Fourier transform to convert EEG signals from the time domain to the frequency domain. This method focuses on the frequency components of the signal, providing insights into different types of brain activity based on their frequency ranges [55], [56]. The relevant methods include: 1. Power spectral density (PSD): Estimating the power of each frequency component to identify major brain rhythms (e.g., delta, theta, alpha, beta, and gamma waves). 2. Band power: Quantifying power within specific frequency bands to study different brain states (e.g., increased alpha power during relaxation). 3. Harmonic analysis: Studying harmonics or multiple frequencies related to the fundamental frequency, revealing complex brain activities.

Time-frequency analysis combines time-domain and frequency-domain methods to examine how the frequency content of EEG signals changes over time. This method provides a more detailed view of the dynamic characteristics of brain activity [57]. The relevant methods include: 1. Short-time Fourier transform (STFT): Dividing EEG signals into short time windows and applying Fourier transform to each window to obtain time-frequency representation. 2. Wavelet transform: Analyzing EEG signals using wavelets (localized oscillating functions) at different scales to capture both frequency and time information. 3. Hilbert-Huang transform

(HHT): Decomposing EEG signals into intrinsic mode functions (IMFs) and analyzing their instantaneous frequency changes over time.

Different analysis methods each have their strengths and weaknesses, making them suitable for various applications and research goals. In practical applications, it is often necessary to combine multiple analysis methods to comprehensively understand and interpret EEG signals. Time-domain analysis allows for direct observation of signals on the time axis, making it easy to understand and interpret. It is straightforward to operate and suitable for real-time monitoring and initial analysis. However, its ability to analyze periodicity and spectral features is limited, making it challenging to reveal frequency components and handle complex, non-stationary signals. Frequency-domain analysis provides detailed information about the frequency characteristics of signals, identifies the energy distribution of different frequency components, and is suitable for long-term trend analysis and spectral feature research. However, it disregards time information and cannot analyze how frequency components change over time, making it less effective for non-stationary signals. Time-frequency analysis simultaneously examines both time and frequency characteristics of signals, providing dynamic information about changes in both domains. It is suitable for analyzing complex and non-stationary signals, capturing short-term changes, and studying variations in brain activity during cognitive tasks, motor activities, or sleep stages. However, it involves high complexity in analysis, requires substantial computational resources, and the selection of time windows and resolution parameters can affect the results.

1.4.2. Nonlinear analysis methods

The theory of nonlinear dynamical systems has advanced to the point where it can be used to study the self-organization and pattern formation of complex neuronal networks in the brain. Through nonlinear time series analysis, attractors of the underlying dynamical system can be reconstructed from the EEG time series and characterized by their dimensions (an estimate of the system's degrees of freedom), Lyapunov exponents, and entropy (reflecting the unpredictability of dynamics due to sensitive dependence on initial conditions) [58]. Recently developed nonlinear measurement methods can also characterize other features of local brain dynamics, such as predictability, time asymmetry, and determinism, as well as the nonlinear synchronization between recordings from different brain regions.

Nonlinear time series analysis can be applied to EEG and MEG data from healthy subjects during task-free resting states, sensory processing, cognitive task execution, and different sleep stages [59]. Using the concepts of "functional sources" and "functional networks" to interpret these results, three basic patterns of brain dynamics can be identified: 1. Normal, persistent dynamic features in healthy subjects during task-free, resting states; 2. Hypersynchronous, highly nonlinear dynamics during epileptic seizures; 3. Degenerative brain pathological dynamics, characterized by abnormally low levels of inter-regional synchronization.

The brain is a complex network composed of coupled and interacting subsystems. Its higher functions, especially cognitive functions, rely on the effective processing and integration of

information within this network. Nonlinear EEG analysis is widely used to study the cortical dynamics underlying various types of cognitive processing [60]. These studies investigate whether brain dynamics become more or less complex during cognitive tasks and attempt to relate changes in the complexity of brain dynamics to the nature and complexity of the tasks and the cognitive levels of the subjects. Additionally, nonlinear methods are used to explore changes in functional interactions between brain regions. Compared to linear methods, nonlinear measurement techniques may be more effective in understanding functional interactions between brain regions during cognitive processing.

1.5. Complex network analysis of EEG

1.5.1. Functional connectivity

Different neurons and brain regions are interconnected in various ways, creating a highly complex and extensive brain network. Modern neuroscience research indicates that many higher cognitive functions rely on the collaboration between different brain regions rather than being dependent on a single specific region. Moreover, the mechanisms of many neurological and psychiatric disorders (such as schizophrenia and depression) can, to some extent, be understood as abnormalities in the connections between these regions. Brain connections can be categorized into three types: structural connectivity, functional connectivity, and effective connectivity.

Structural connectivity refers to the anatomical connections between neurons or brain regions, such as axonal or synaptic connections between neurons, and neural fiber bundles connecting cortical and subcortical structures [61]. Functional connectivity is assessed using

signals recorded from different brain regions (e.g., BOLD signals from MRI, EEG, or MEG signals) and reflects the strength of the relationship between these regions. The simplest measure of this relationship is the Pearson correlation coefficient, although more complex measures also exist [62]. Effective connectivity, on the other hand, represents a causal influence and has a directional nature [63]. For example, if there is an anatomical connection between neuron A or brain region A and neuron B or brain region B, and neuron A or brain region A can send commands to neuron B or brain region B, this connection is directional and falls under effective connectivity. Additionally, if the method used to calculate functional connectivity from the recorded signals involves a causal measure such as Granger causality, then the resulting functional connectivity is also considered effective connectivity. In summary, effective connectivity is a specific subset of both structural and functional connectivity.

EEG functional connectivity refers to the method of recording brain activity using electrophysiological measures, which reflect changes in electrical potentials due to synchronous neural activity [64], [65]. This approach provides a time-correlated analysis of the electrophysiological activities of brain cells, revealing the information exchange and functional connections between different regions. Various indices are used in EEG functional connectivity analysis, each with specific applications and strengths. Common methods include: 1. Pearson correlation coefficient: One of the simplest functional connectivity indices, used to measure the linear correlation between two signals. 2. Spectral coherence: Measures the correlation between two signals in the frequency domain. 3. Mutual information: An information theory-based method that quantifies the amount of information one signal

contains about another. 4. Phase locking value (PLV): A phase-based functional connectivity method that measures the phase synchronization between two signals. 5. Phase lag index (PLI): Similar to PLV, used to measure phase synchronization between two signals, less sensitive to volume conduction effects but potentially more sensitive to noise. 6. Partial directed coherence (PDC): A multivariate effective connectivity measure based on Granger causality, assessing the causal influence between signals with directional properties.

1.5.2. Complex network theory

For centuries, the debate between the localization and integration of brain function has been intensely contested, with integration emerging as the dominant perspective in recent decades. Adding to the complexity is the inherently multi-scale nature of neural functions, which range from synaptic connections of individual cells to organized assemblies within local anatomical regions, and extend to large-scale structures of brain regions interconnected by neural pathways [66]. While the anatomical structure of synapses and pathways inevitably constrains brain network functions, research has demonstrated that brain regions do not need to be directly physically or structurally connected to exhibit their functional properties. Furthermore, dynamic changes in functional networks can remodel the physical structure of brain networks through plasticity. Network science offers theoretical foundations and analytical tools for data-driven, quantitative assessments of brain function. It enables the inference of network models from experimental data and the modeling of coupling between brain systems, as well as their modulation by tasks, sensory stimuli, or time, without presuming how different brain regions participate in various cognitive processes.

Estimating brain functional networks from experimental data typically involves the following steps. Nodes in the network are defined based on the underlying brain anatomy and the sensing technology used, and statistical dependencies between the time series signals generated by node pairs are estimated. Depending on the type of measurement used, functional connectivity networks can be directed or undirected, reflect linear or nonlinear functional coupling, involve bivariate or multivariate effects, and operate in the time or frequency domain [67], [68]. Next, these estimates are organized into an adjacency matrix for further analysis. The rows and columns of the adjacency matrix represent the network nodes, and the entries correspond to the values estimated using statistical dependency measures. The adjacency matrix is often sparsified through a thresholding process that removes weak connections, with the threshold varying to observe its impact on the results. However, recent studies have indicated that this method may excessively remove weak connections that could have functional relevance. Therefore, biologically relevant thresholding criteria based on maximizing information flow rather than wiring cost have been proposed. In the final step, the processed adjacency matrix is used to calculate graph theory metrics that characterize the connectivity network embedded in the examined data. This step is typically accompanied by statistical analysis to determine the significance of observations compared to a random network baseline.

1.5.3. Node and edge of complex network

The definition of nodes largely depends on the sensing modality. Broadly speaking, nodes can be categorized in three different ways: 1. In the measurement space after image reconstruction, in voxel-based modes such as fMRI or PET. 2. In the electrophysiological

modes (EEG and MEG), as well as in the sensor space of fNIRS. 3. Based on source reconstruction techniques for EEG and MEG.

In voxel-based modes, the main consideration is the spatial scale most relevant to subsequent analysis, which determines whether to consider individual voxels or groups of voxels (ROIs) [69]. Early brain network analysis methods used individual voxels to describe nodes. While this method may offer higher resolution than ROI-based methods and naturally supports model-free analysis, it has a lower signal-to-noise ratio and results in high-dimensional networks compared to ROI-based analysis. When using ROI-based methods, further choices must be made regarding how to aggregate voxels: brain segmentation based on anatomical atlases, data-driven segmentation, or mixed methods [70]. Due to increasing detail in brain anatomical knowledge and improving resolution of neuroimaging techniques, network scales have become unsustainable. Consequently, it is not surprising that most current methods are ROI-based. Researchers use prior anatomical knowledge from atlases such as the Automated Anatomical Labeling (AAL3) atlas, brain anatomical labels, Brodmann areas based on cellular structure information, or the LONI probabilistic atlases [71], [72], [73], [74]. Recent methods also use connectivity information for segmentation, based on the idea that each functionally specialized brain region has a specific pattern of connections with other regions, thereby defining its function. The choice of segmentation method, the atlas used for voxel registration, and the number of network nodes all significantly impact the derived graph measures and the ability to compare results across studies [75]. Therefore, when comparing topological measures of brain networks, it is recommended to use similar spatial scales (in

terms of the number of nodes). Another commonly used method for representing nodes as voxel groups is Independent Component Analysis (ICA). This method maps each independent component (IC) to a distributed region and constructs an adjacency matrix reflecting functional connectivity based on IC time series [76]. The number of ICs depends on the nature of the functional process under study, ranging from fewer than 10 to 50 or more.

In sensor-based modes, brain network nodes are typically represented directly by sensors or electrodes. This greatly simplifies the network construction process; however, due to volume conduction phenomena and sensor grid layouts, signals recorded by each sensor or electrode do not directly represent the electrical activity of neural regions but rather simultaneous activities from multiple cortical sources. Although most current EEG and MEG studies ignore these factors, several methods can address these issues. The first method involves using spatial filters, primarily based on Laplace algorithms, to remove common components from signals recorded by a set of neighboring electrodes [77]. The second method includes using functional connectivity estimation techniques that account for volume conduction effects, such as the phase lag index or imaginary coherence [78]. Another approach used in EEG and MEG-derived networks defines network nodes as cortical sources assumed to generate the recorded scalp signals [79]. These sources are estimated using complex source localization techniques by solving an inverse problem. Such techniques can be based on regularized least squares algorithms, Bayesian methods, tensor-based methods, or extended source scanning methods such as beamforming.

Additionally, for EEG and MEG, signals can be decomposed into typical frequency bands using band-pass filtering techniques. This can be done both at the sensor level and the source level once signals corresponding to cortical sources are reconstructed. EEG/MEG frequency bands are classified as delta (1-4 Hz), theta (4-8 Hz), alpha (8-13 Hz), and beta (>13 Hz), while higher frequency activities (usually above 30 Hz) are referred to as gamma activities. In these analyses, different functional connectivity networks are constructed within each frequency band, enabling multilayer network analysis.

After defining the nodes, the next step is to evaluate the statistical dependencies of the neural signals corresponding to the nodes. Many factors need to be considered at this stage, as recent research reviews have identified over 40 methods for estimating functional connectivity [80], [81]. When choosing the most appropriate connectivity measure, the fundamental assumptions of the study must be taken into account. For example, in the context of investigating the response to pain stimuli, it is known that pain is an integrative phenomenon involving interactions between sensory, motor, attention, and other contextual factors. Therefore, if the goal is to investigate the mechanisms activated in attention and motor responses to pain stimuli, using directed connectivity measures will be suitable. These measures theoretically better describe the influence of somatosensory areas on the medial prefrontal cortex, reflecting their causal relationship and its involvement in attention processing. Conversely, if the objective is to study synchronization between distant brain regions during the memory retention phase of a working memory task, undirected functional connectivity measures (such as correlation) will be more appropriate for brain network

analysis [82], [83]. Some measures, such as Granger causality and transfer entropy, provide directed indices because the cause precedes the effect in time. Cross-frequency coupling in complex cognitive processes, such as creative thinking, can be better reflected through frequency domain connectivity measures like phase-amplitude coupling (PAC). Compared to the broad frequency range of EEG/MEG, the lower frequency range somewhat limits the applicability of frequency domain connectivity measures in BOLD signals. Thus, time-domain measures tend to have wider applicability in fMRI and fNIRS.

1.5.4. Network analysis measures

The brain connectivity data includes networks of brain regions connected by anatomical tracts or functional associations. Complex network analysis is a novel multidisciplinary method for studying complex systems, with the goal of characterizing these brain networks using a small number of neurobiologically meaningful and computationally feasible measures [84], [85]. Network approaches have been extended to various aspects of neuroscience research. In network studies, characterizing the topological relationships of complex networks using graph theory is a crucial method for investigating the properties of different nodes, edges, and overall network characteristics.

Modern brain mapping techniques have generated increasingly large datasets of anatomical or functional connectivity patterns. Concurrent technological advancements are producing similar large-scale connectivity datasets in biology, technology, social sciences, and other fields [86], [87]. Over the past decade, efforts to describe these datasets have led to the emergence of a new multidisciplinary approach for studying complex systems, known as

complex network analysis. This approach characterizes important aspects of complex systems by quantifying the topology of their respective network representations. Although complex network analysis originated from graph theory, it primarily deals with large and complex real-world networks that are neither uniformly random nor orderly, distinguishing it from classical graph theory.

Brain connectivity datasets consist of networks of brain regions connected by anatomical tracts or functional associations. Brain networks are inherently complex and share many characteristics with networks in other biological and physical systems, making complex network methods applicable for their characterization [66]. The analysis of structural and functional connectivity data in networks is increasing, driven by several key motivations. First, complex network analysis provides a reliable means of quantifying brain networks using a small number of neurobiologically meaningful and computationally feasible measures. Second, by clearly defining anatomical and functional connections on the same brain region map, network analysis offers a useful framework for exploring structure-function connectivity relationships. Third, comparing the topological structures of structural or functional networks between study groups can reveal presumed connectivity abnormalities in neurological and psychiatric disorders. In practical research, however, researchers often select network properties tailored to their specific research objectives. Moreover, as graph theory methods evolve, many new metrics continue to emerge, including degree, assortativity coefficient, characteristic path length, betweenness centrality, participation coefficient, modularity, rich club coefficient, global efficiency, and local efficiency. A comprehensive and accurate

understanding of these graph theory metrics is essential for applying graph theory methods to the study of complex networks.

1.6. Current research background

Response inhibition refers to an individual's ability to suppress or delay their response when presented with stimuli. This ability is crucial in daily life and holds significant research value in neuroscience. The neural mechanisms underlying response inhibition can be explored through various experimental paradigms, with the Go/No-Go task being particularly effective for assessing this ability [17], [88]. This task typically involves two types of stimuli: Go stimuli, which require a response, and No-Go stimuli, which require response inhibition. Previous studies have examined response inhibition using equal numbers of Go and No-Go conditions or specific proportions, such as 7:3. However, how the ratio of Go to No-Go conditions affects the underlying mechanisms of response inhibition remains unclear.

Reaction times serve as a genuine measure to assess the underlying psychological mechanisms relevant to a psychological experiment. In Go/No-Go experiments, reaction times to Go stimuli serve as an indicator of the involvement of inhibition processes, exploring the efficiency of inhibition. Slower reaction times to Go stimuli are associated with a higher probability of successful inhibition trials, while faster reaction times increase the likelihood of inhibition trial failures. Kok et al.'s study suggests that assumptions regarding the timing and nature of inhibition processes are primarily validated temporally, proving to be reasonable [52]. Several other studies also indicate that models based on reaction times in Go/No-Go tasks contribute to the interpretability and effectiveness of measuring inhibition mechanisms.

Currently, the interpretation of how reaction times to Go stimuli in Go/No-Go tasks under different ratio conditions elucidate inhibition mechanisms is still under exploration.

Event-related potentials (ERPs) allow us to understand how the brain processes different types of stimuli and provide information about individual brain activity during tasks. Currently, there is controversy surrounding ERP studies of response inhibition, and the brain mechanisms associated with response inhibition have been investigated [89], [90], [91]. It is generally believed that areas such as the frontal cortex play key roles in the process of response inhibition. The positive components around 300 ms (P3) are commonly seen as markers of how the brain evaluates and processes stimuli. Variations in the P3 component indicate the degree to which the brain processes different types of stimuli and allocates cognitive resources relevant to the task [92]. Frontal No-Go-related P3 components have been widely studied in response inhibition research, although some early studies did not specifically emphasize the relationship between the P3 component and response inhibition. However, recent studies have indicated that central P3 components related to No-Go conditions are associated with the process of response inhibition. For example, Albert et al.'s ERP study explored a modified Go/No-Go task with stimuli of three different frequency types [52]. The results revealed a greater amplitude of the central P3 in No-Go trials under infrequent conditions compared to Go trials under the same conditions. However, this experiment did not focus on the influence of different Go and No-Go ratio conditions on response inhibition. The different proportions of Go and No-Go stimuli are closely related to the brain's motor planning and execution, which are crucial for regulating the ability and speed

of inhibitory response actions. These processes involve several functional brain areas, such as the primary motor cortex (M1), the pre-motor cortex (PMC), and the supplementary motor area (SMA), which are concentrated in the central region of the brain. The use of ERP technology allows for the capture of relevant brain activity and the differences in brain activity brought about by different proportion conditions. Therefore, the present study focused on analyzing the P3 components in central regions and investigating the effects of different ratios of Go and No-Go stimuli on these ERP components.

In the Go/No-Go task paradigm, the ratio of Go to No-Go stimuli influences participants' predictions of stimuli and their ability to inhibit responses, thereby affecting cognitive control and executive function performance [93]. For example, when the paradigm includes a higher ratio of Go stimuli, participants are more likely to expect the next stimulus to be a Go stimulus during cognitive processing, making it easier to respond accordingly. Conversely, when the ratio of No-Go stimuli is greater, participants may more frequently anticipate the next stimulus to be a No-Go stimulus, making it easier to inhibit responses [94]. According to Bayesian brain theory, the brain forms expectations about stimuli and adjusts responses accordingly through stimulus recognition and learning from prior experiences [95], [96]. The human prediction mechanism is based on constantly updating previous knowledge according to new experiences. When external stimuli match expectations, the predictive mechanism strengthens the relevant responses, thereby promoting effective behavioral control. This mechanism plays a crucial role in various cognitive processes, including response inhibition. In Go/No-Go tasks, the ratio of Go to No-Go stimuli is considered a prior probability,

representing the initial estimate of the occurrence of different types of stimuli. Therefore, exploring the ratio or probability distribution of Go and No-Go conditions may be valuable in studying the impact of prediction on response inhibition.

Moreover, regarding the dynamic characteristics of brain activity related to response inhibition, our investigation revealed that no current studies have employed complex network analysis to explore the dynamic features of EEG data, likely due to the novelty of this methodology. Complex network analysis offers a new approach to understanding functional connectivity patterns in the brain under different task conditions. While traditional ERP analysis primarily focuses on neural activity at specific time points, complex network analysis can uncover dynamic changes across the entire brain network during task execution.

1.7. Research Goals

Overall, we aimed to modulate the difficulty of the modified Go/No-Go task by introducing directional cues. The high temporal resolution of ERP components allows us to examine millisecond-level dynamic neural activity. In the experiments, we considered four ratio conditions: 100%:0%, 75%:25%, 50%:50%, and 25%:75% proportions of Go and No-Go stimuli. Participants were informed of the specific distribution in the task description before starting. The experimental task required participants to determine whether the cues and target stimuli were aligned in the same direction. Consistent directions indicated Go trials, while inconsistent directions indicated No-Go trials. 1. In behavioral experiment, we set ISI and ratio as two independent variables to explore whether ISI and Go/No-Go ratio have a statistically significant impact on Go reaction time, with ISI being a parameter in the

experimental design. 2. Based on the behavioral experiment, we selected a fixed ISI and analyzed ERP components to investigate the impact of different ratios on the neural mechanisms of response inhibition. we analyzed the reaction time in the Go trials and the error rate in the No-Go trials under different conditions, indicating the influence of prior probability on reaction control. We also analyzed the ERP components, especially the amplitude and latency of the NoGo-P3 component of the central area. The NoGo-P3 component effectively reflects the reaction inhibition process. 3. Based on the ERP experiment, we conducted a complex network analysis of the collected whole-brain EEG data to explore the impact of Go/No-Go ratio on response inhibition from the perspective of the overall and dynamic characteristics of functional network connectivity.

2. Behavioral Experiment

2.1. Materials and Methods

2.1.1. Participants

Twenty individuals (10 males and 6 females), aged between 20 and 30 years (with a mean age of 22.75 ± 0.78 years, mean ± SD; all right-handed), volunteered for the experiment. None of the participants had a documented history of major medical or neurological issues, such as loss of tactile sensation, epilepsy, severe head injuries, or chronic alcohol dependency. Before participating in the study, all participants provided written consent. The study protocol was reviewed and approved by the local medical ethics committee at Okayama University in Japan.

2.1.2. Stimuli and procedures

We employed a Go/No-Go task as the experimental paradigm. The experiment was conducted in a soundproof chamber using a motion-controlled setup with a 4-way joystick fixed to the right-hand side of the participants. The experimental stimuli were displayed on a screen located 60 cm from the participants. The paradigm was implemented using MATLAB R2021b, as illustrated in Figure 1. Initially, a black central cross was shown for 1200 ms against a gray background (R:127, G:127, B:127), followed by a randomly oriented green equilateral triangle as a visual cue. The time interval between the cue and the target (ISI) was set to 100 ms, 300 ms, or 500 ms. Subsequently, another randomly oriented green equilateral triangle was presented as the target. After the target appeared, participants were required to make an immediate judgment: if the cue and target directions matched, it was considered a

"Go" response; otherwise, it was a "No-Go" response. In the "Go" scenario, participants were instructed to swiftly move the joystick in the direction of the target, while in the "No-Go" scenario, no action was required. A fixed intertrial interval of 2600 ms followed the presentation of each target.

The experiment consisted of 8 blocks, with each ratio condition having three ISI conditions. Each combination of ratio and ISI conditions included 60 trials, resulting in a total of 180 trials per block. The order of the blocks was randomized. Prior to the start of each block, participants were not informed of the 'Go' and 'No-Go' stimulus ratio. Following the completion of each block, participants were given appropriate rest intervals.

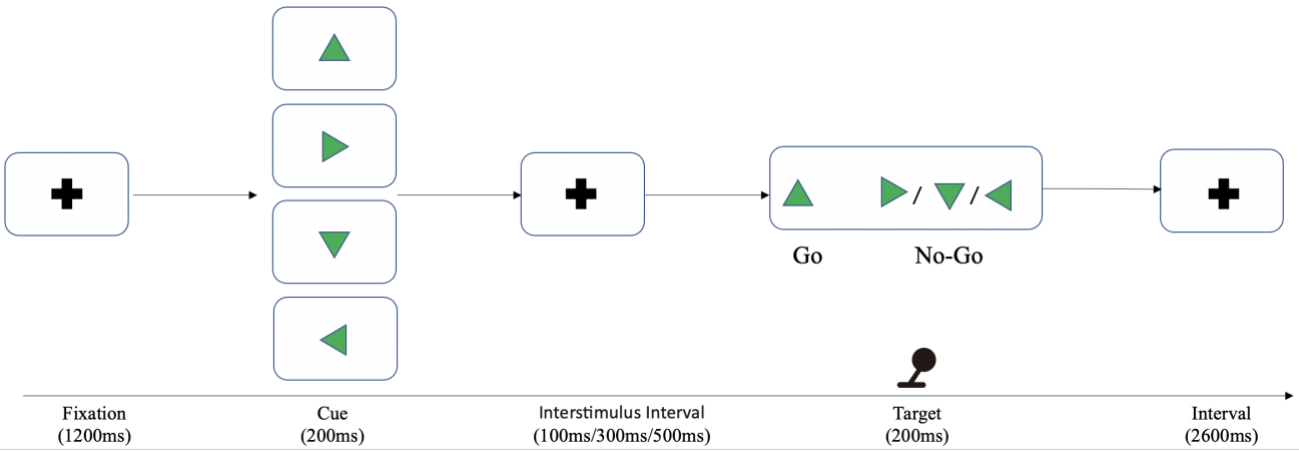

Figure 1. Behavioral experimental paradigm. The participants were instructed to promptly assess both stimuli after the presentation of the cue and target. In the "Go" trials, the direction of the stimuli matched, and the joystick on the right-hand side was to be moved in the stimulus direction. In the "No-Go" trials, the directions of the stimuli did not match, and the participants were instructed to refrain from making any movements.

2.1.3. Statistical analysis

For behavioral data, we compared the mean reaction times in the Go trials under different conditions. To investigate the two-way interaction between ISIs and the ratios of Go and No-Go stimuli, we conducted a repeated-measures ANOVA. Post hoc analysis was performed with Bonferroni correction. Statistical significance was accepted at $p<0.05$. Unless otherwise stated, all results are presented as the mean ± MSE (mean squared error).

2.2. Results

The distribution of Go reaction times across different conditions is shown in Figure 2. We conducted a repeated measures ANOVA on the reaction times for the Go trials under different conditions. The results indicated a strong main effect of the different Go and No-Go trial ratios, F (3.15, 48.26) = 306.89, p < 0.001. However, there was no significant statistical difference in Go reaction times between the different ISI conditions, p = 0.093. Additionally, there is no interaction effect between the ISI and ratio variables.

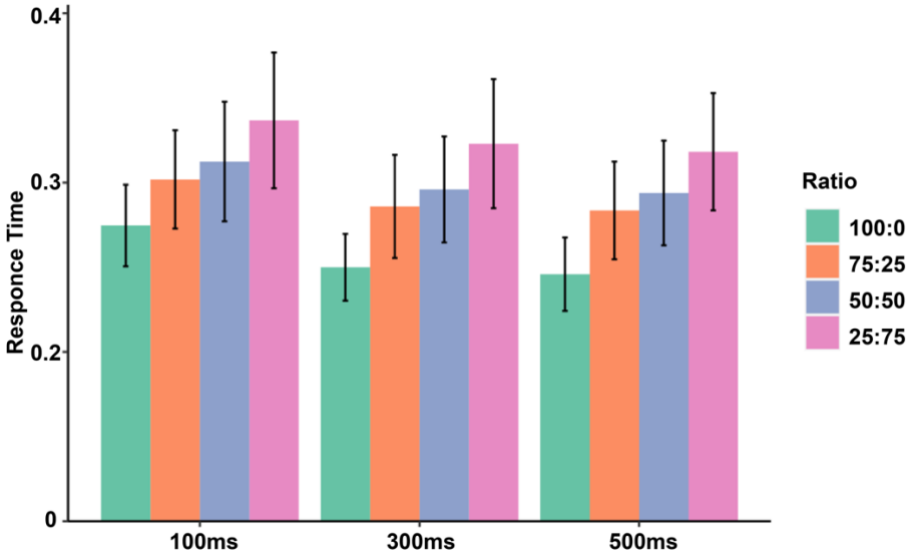

Figure 2. Performance of Go reaction times. The three bar graphs correspond to different ISI conditions,

from left to right: 100 ms, 300 ms, and 500 ms. Different colors represent different ratio conditions, with green for 100:0, orange for 75:25, purple for 50:50, and pink for 25:75. Under different ISI conditions, the Go trial reaction times show a trend of increasing as the proportion of Go trials decreases.

The statistical differences in Go response times under different ratio conditions are shown in Figure 3. Under various ratio conditions, Go response times increase with the number of Go trials. For an ISI of 100 ms, significant statistical differences were observed between the 100:0 and 50:50 conditions (p=0.011) and between the 100:0 and 25:75 conditions (p<0.001). A significant difference was also found between the 75:25 and 25:75 conditions (p=0.023). For an ISI of 300 ms, significant differences were observed between the 100:0 and 25:75 conditions (p=0.009), between the 100:0 and 50:50 conditions (p<0.001), and between the 100:0 and 25:75 conditions (p<0.001). Additionally, a significant difference was found between the 75:25 and 25:75 conditions (p=0.007). For an ISI of 500 ms, significant differences were observed between the 100:0 and 25:75 conditions (p=0.004), between the 100:0 and 50:50 conditions (p<0.001), and between the 100:0 and 25:75 conditions (p<0.001). Furthermore, a significant difference was found between the 75:25 and 25:75 conditions (p=0.009). These results indicate that as the ISI duration increases, the differences between the ratios become more significant.

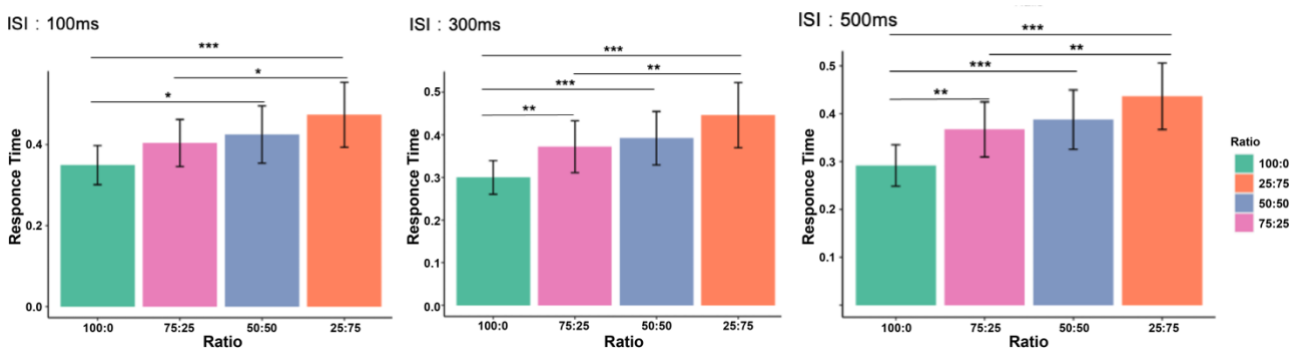

Figure 3. Statistical differences among different ratio conditions under each ISI. (*p < 0.05, **p < 0.01, ***p < 0.001).

Statistical differences between different ISI conditions are shown in Figure 4. We found that significant statistical differences were only present when the ratio of Go to No-Go trials was 100:0, between ISIs of 100 ms and 300 ms, as well as between 100 ms and 500 ms, with p=0.008 and p=0.002 respectively. Additionally, under any ratio condition, there were almost no changes in Go reaction time between 300 ms and 500 ms.

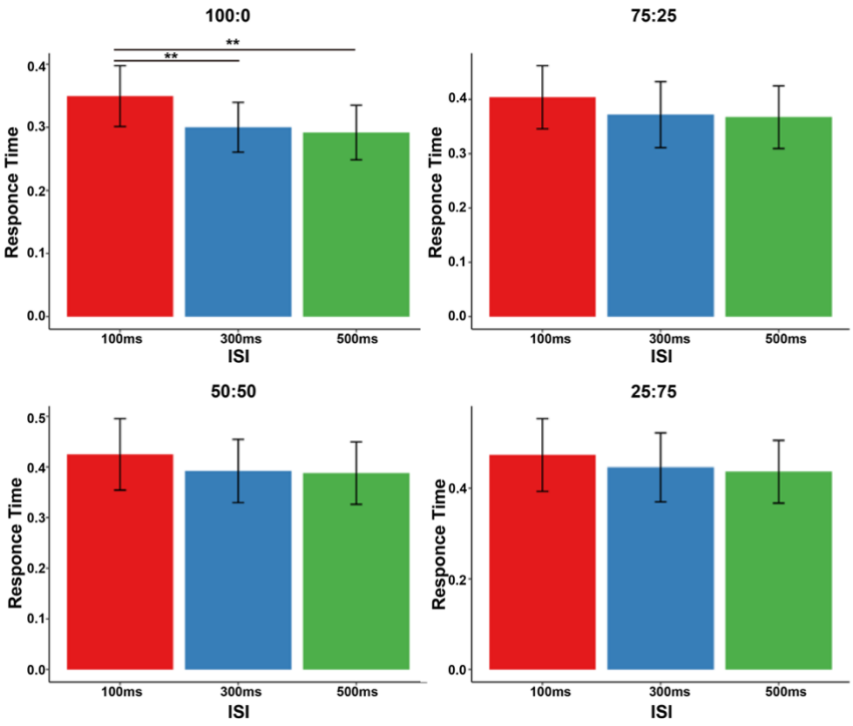

Figure 4. Statistical differences among different ISI conditions under each ratio of Go and No-Go. (*p < 0.05, **p < 0.01, ***p < 0.001).

2.3. Discussion

In this study, we explored the effects of Go and No-Go ratios, as well as ISI, on response inhibition in a Go/No-Go experiment. The results indicate that the ratio of Go to No-Go trials influences the reaction times of Go trials; specifically, as the number of Go trials decreases, reaction times increase. The time interval between cues and targets did not have a statistically significant effect on the reaction times of Go trials, but the results show that reaction times tend to stabilize after 300 ms. There was no significant interaction between the ratios of Go and No-Go trials and the time interval between cues and targets.

2.3.1. Different ISI impact on response inhibition

ISI settings play a crucial role in studying response inhibition in cue-target tasks. Different ISI settings can influence participants' expectations and the effectiveness of response inhibition. Under shorter ISI conditions, participants may rely on short-term memory and make quick decisions, leading to higher rates of response inhibition errors. In contrast, longer ISI conditions may provide participants with more time for information processing and response preparation, thereby enhancing the accuracy of response inhibition [17], [97]. Research indicates that different ISI conditions can also significantly affect ERP components, such as the amplitude and latency of NoGo-P3, reflecting adjustments in the brain's neural mechanisms for response inhibition under various temporal conditions. Exploring the impact of different ISI conditions on response inhibition helps deepen our understanding of the brain's temporal dynamics and cognitive control mechanisms.

Specifically, a 100 ms ISI represents a short interval condition associated with attentional

priming [98]. During short intervals, cues can effectively guide attention to upcoming targets, thereby reducing reaction times. The brief interval allows attention to quickly shift and focus on the target stimulus, contributing to faster responses. A 300 ms ISI falls under moderate interval conditions, likely involving the reallocation of attentional resources. Within this interval, there may be a redistribution of attentional resources as the influence of the cue diminishes, requiring additional time to adjust attention for the imminent target stimulus. Reaction times typically fall within a moderate range, between the shortest and longest intervals. A 500 ms ISI represents a long interval condition, potentially accompanied by attentional decay [99]. Extended intervals cause the cue's influence to gradually diminish, necessitating more time to redirect attention toward the target stimulus. Consequently, reaction times tend to be relatively longer as more time is required to shift focus from the cue to the target stimulus.

In our study, stable trends were observed in Go trial responses at intervals of 300 ms and above, with no statistically significant differences. This consistency aligns with cognitive psychology principles of attentional regulation and information processing mechanisms. At intervals of 300 ms and above, participants have sufficient time to recover from the cue's influence and reallocate attention effectively toward the impending target stimulus. This process remains stable and effective, without significant reaction time differences due to slightly longer intervals. As intervals increase, participants have more time to prepare for and anticipate the appearance of the target stimulus. This preparation process tends to proceed smoothly, without causing significant reaction time differences despite intervals exceeding 300 ms. For most cognitive tasks, intervals of 300 ms and above provide ample time for

attentional shifting and information processing, resulting in minimal observable differences in reaction times within this temporal range.

2.3.2. Different ratio impact on response inhibition

Adjusting the ratio of different stimulus types is widely applied in psychological experiments across various research topics. Modulating the ratio of stimulus types helps researchers explore mechanisms of cognitive control, especially in response to frequently versus infrequently occurring stimuli [100], [101]. Ratio conditions reveal participants' strategies for response inhibition under different cognitive loads. Designing stimuli with varying proportions influences participants' attentional allocation strategies. Under high ratio conditions, participants may prioritize and quickly respond to frequently occurring stimuli, whereas under low ratio conditions, more attentional resources may be needed to monitor and inhibit less common stimuli. This design aids in understanding the dynamic adjustments of attention during cognitive tasks. Modulating stimulus type ratios provides insights into decision-making processes [102]. Participants adjust their decision-making strategies and response styles when confronted with different ratios of stimuli, revealing underlying psychological processes and strategy choices. Additionally, ratio conditions can be utilized to study the impact of different stimulus ratios on neural activity, such as event-related potentials (ERPs). For instance, ratio conditions can elucidate changes in neural activity (e.g., NoGo-P3) under different stimulus ratios, aiding in the understanding of neural response mechanisms under varying cognitive loads. Adjusting the ratio of different stimulus types is an important experimental design tool in the study of cognitive processes, providing a robust method for understanding complex cognitive functions. Research on response inhibition associated with

ratios primarily investigates the effects of different attentional or memory loads by setting fixed ratios [103], [104]. However, our study investigates the regulatory effects of different ratio conditions on response inhibition ability, a topic that has not been extensively explored in previous research.

The Go/No-Go task is widely used in studies of response inhibition, where the reaction time to Go trials has been validated as a quantifiable measure of response inhibition ability. Changes in reaction times associated with different ratio variations demonstrate the regulatory effect of ratio conditions on response inhibition ability. Research findings indicate a statistically significant trend of increased reaction times as the number of Go trials decreases. The modulation of ratio conditions is related to brain prediction mechanisms; participants learn about the ratio information during experiments and use this experience as prior information to predict and judge forthcoming stimuli. This predictive process requires additional time for information processing and may involve prediction errors [105]. The regulatory effect of ratio information on response inhibition can be quantified by examining reaction times to Go trials in Go/No-Go tasks, which is crucial for a deeper exploration of response inhibition mechanisms based on these foundations.

2.4. Conclusion

In this study, we explored the effects of different Go and No-Go trial ratios and interstimulus intervals (ISIs) on response inhibition in Go/No-Go experiments. The ratio of Go to No-Go trials significantly influenced the reaction times of Go trials; specifically, as the proportion of Go trials decreased, reaction times increased. The study found no significant interaction

between the ratios of Go and No-Go trials and ISI, indicating that these factors independently affect response inhibition processes. Although ISI settings did not show statistically significant effects on response inhibition in this study, different ISI intervals revealed stable results in Go trial responses, particularly at intervals of 300 ms or more. Overall, these findings underscore the importance of considering ratio conditions and ISI settings when studying response inhibition and cognitive control mechanisms. They provide insights into how experimental designs can deepen our understanding of complex cognitive processes and neural dynamics in Go/No-Go tasks.

3. ERP Experiment

3.1. Materials and Methods

3.1.1. Participants

Twenty individuals (14 males and 8 females) aged between 20 and 30 years (mean age: 24.68 ± 3.15 years, mean ± SD; all right-handed) volunteered for the experiment. None of the participants had a documented history of major medical or neurological issues, such as loss of tactile sensation, epilepsy, severe head injuries, or chronic alcohol dependency. Before participating in the study, all participants provided written consent. The study protocol was reviewed and approved by the local medical ethics committee at Okayama University in Japan.

3.1.2. Stimuli and procedures

We employed a Go/No-Go task as the experimental paradigm. The experiment was conducted in a soundproof chamber using a motion-controlled setup with a 4-way joystick fixed to the right side of the participants. The experimental stimuli were displayed on a screen positioned 60 cm from the participants. The paradigm was implemented using MATLAB R2021b, as depicted in Figure 5. Initially, a black central cross was presented for 1200 ms against a gray background (R:127, G:127, B:127), followed by a randomly oriented green equilateral triangle as a visual cue. The time interval between the cue and the target was set at 500 ms. Subsequently, another randomly oriented green equilateral triangle was presented as the target. After the target appeared, participants were required to make an immediate judgment: if the cue and target directions matched, it was considered a "Go" response;

otherwise, it was considered a "No-Go" response. In the "Go" scenario, participants were instructed to swiftly move the joystick in the indicated direction, while in the "No-Go" scenario, no action was required. A fixed intertrial interval of 2000 ms followed each target presentation.

The experiment comprised 8 blocks structured as follows: blocks 1 and 2 included 100% Go trials, blocks 3 and 4 included 75% Go trials, blocks 5 and 6 included 50% Go trials, and blocks 7 to 8 included 25% Go trials. The distribution of Go and No-Go trials for each block was as follows: blocks 1 and 2 (Go: 144, No-Go: 0), blocks 3 and 4 (Go: 108, No-Go: 36), blocks 5 and 6 (Go: 72, No-Go: 72), and blocks 7 and 8 (Go: 36, No-Go: 108).

The order of the blocks was randomized. Prior to the start of each block, participants were informed of the ratio of 'Go' to 'No-Go' stimuli. Following the completion of each block, participants were provided with appropriate rest intervals.

Paradigm:

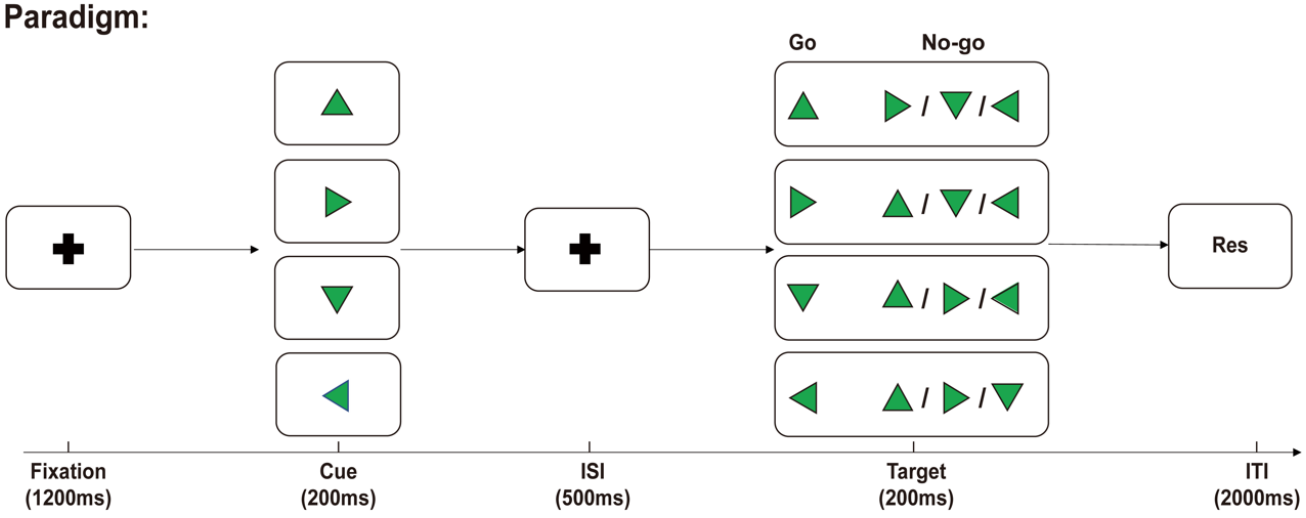

Figure 5. ERP Experimental paradigm. The participants were instructed to promptly assess both stimuli after the presentation of the cue and target. In the "Go" trials, the direction of the stimuli matched, and the joystick on the right-hand side was to be moved in the stimulus direction. In the "No-Go" trials, the

directions of the stimuli did not match, and the participants were instructed to refrain from making any movements.

3.1.3. EEG recording and preprocessing

The EEG signals were recorded with reference to the left mastoid using a 64-channel amplifier with a sampling frequency of 1000 Hz (Brain Products, Germany). The ground electrode was integrated into the cap on the medial frontal aspect. Two additional electrodes were placed approximately 1.5 cm from the left outer canthus and above the right eye to record horizontal and vertical electrooculograms (EOGs), respectively. EEG data were collected with electrode impedances maintained below 5 kΩ.

EEG preprocessing was conducted using the EEGLAB (Version 2023.1) and ERPLAB toolboxes (Version 10.01) in MATLAB R2021b. The raw EEG data were bandpass filtered between 0.1 and 30 Hz. Independent component analysis was employed to correct for ocular artifacts. Subsequently, continuous EEG data were downsampled to 500 Hz and re-referenced to the average of all electrodes. EOG artifacts were removed. The continuous EEG data were then segmented from -200 to 800 ms relative to the target. Artifact detection using ERPLAB was performed on all EEG epochs, examining the maximum allowable amplitude difference (threshold: ±100 μV) among all EEG channels within a moving window using the peak-to-peak function. Following artifact rejection, the excluded trials accounted for less than 10% of the total trials, and the number of trials did not significantly differ across experimental conditions.

3.1.4. Statistical analysis

Repeated-measures analysis of variance (ANOVA) was used to compare behavioral data and the amplitude and latency of the P3 component at the average of the central electrodes (Cz, C1, C2, FCz, FC1, FC2, PCz, PC1, PC2) using SPSS 26.0. Correct responses in the Go and No-Go trials were of interest. If Mauchly's test of sphericity was violated, the degrees of freedom were adjusted using Greenhouse–Geisser correction. For behavioral data, we compared the mean reaction times in the Go trials and the error rates in the No-Go trials under different ratio conditions. The time window for the NoGo-P3 component at the average of the central electrodes was set between 300 ms and 400 ms, with Bonferroni corrections applied for multiple comparisons. Statistical significance was accepted at $p < 0.05$. Unless otherwise stated, all results are presented as the mean ± MSE (standard error of the mean).

3.2. Results

3.2.1. Behavioral performance

We conducted repeated-measures ANOVA based on the reaction times in all correct Go trials under the four different Go and No-Go ratio conditions (with Go trial ratios of 100%, 75%, 50%, and 25%). The statistical analysis results showed that the main effect of the reaction time in the Go trials across the four conditions was significant (F (2.177, 21.775) = 59.723, $p < 0.001$, $\eta_p^2 = 0.857$), with significant differences observed between any two conditions. As depicted in Figure 6a, the shortest reaction times were observed with a Go trial ratio of 100%, with the reaction time gradually increasing as the ratio decreased. Compared to the 100% Go condition, the reaction times were significantly increased in the 75% (t (21) = 5.830, $p < 0.001$, d = 1.758), 50% (t (21) = 8.850, $p < 0.001$, d =2.668), and 25% conditions (t (21) =

11.024, $p < 0.001$, $d = 3.324$). Moreover, the reaction times in the 75% (t (21) = 6.286, $p < 0.001$, $d = 1.895$) and 50% (t (21) = 4.932, $p < 0.001$, $d = 1.487$) conditions were significantly shorter than that in the 25% condition. Additionally, while the difference in reaction time between the 50% and 75% conditions was not as pronounced, the difference was still statistically significant (t (21) = 2.338, $p = 0.041$, $d = 0.705$).

Furthermore, repeated-measures ANOVA was conducted based on the error rates in the No-Go trials under three different ratio conditions (with Go trial ratios of 75%, 50%, and 25%). The main effect of the error rate in the No-Go trials across the three conditions was significant (F (1.028, 10.280) = 23.21, $p = 0.001$, $\eta_p^2 = 0.699$), with significant differences observed between any two conditions. As illustrated in Figure 6b, the error rates were highest with a Go trial ratio of 75%, and the error rate in this condition was significantly greater than the error rate in the 50% (t (21) = 4.928, $p < 0.001$, d = 0.1.485). and 25% conditions (t (21) = 4.796, $p < 0.001$, $d = 1.446$). Under the 25% condition, the error rate in the No-Go trials was nearly zero, which was significantly lower than that in the 50% condition (t (21) =3.203, p = 0.028, d =0.966).

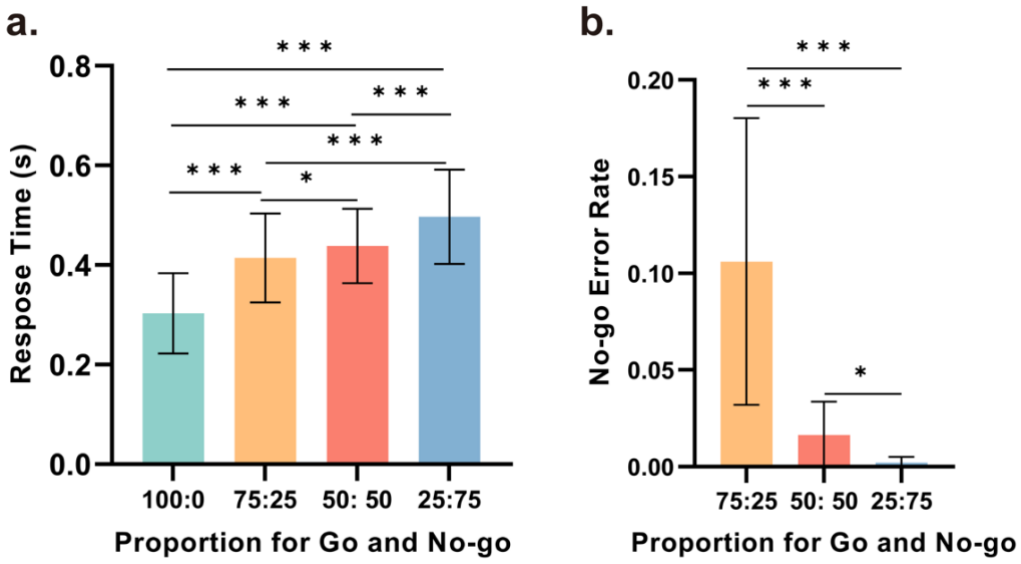

Figure 6. Behavioral performance. (a) A comparison of the reaction times for Go trials between any two ratio conditions revealed statistically significant differences. Reaction times were shortest when Go trials comprised 100% of the trials and longest when Go trials comprised 25% of the trials. Statistical significance was observed for all comparisons between any two conditions. (b) A comparison of the error rate for No-Go trials between any two ratio conditions revealed statistically significant differences. The error rates were highest with a Go trial ratio of 75%, whereas a Go trial ratio of 25% resulted in the lowest error rates. Statistical significance was observed for all comparisons between any two conditions (*$p < 0.05$, **$p < 0.01$, ***$p < 0.001$).

3.2.2. ERP results

For the NoGo-P3 component, as there were no No-Go trials in the 100% condition, we analyzed No-Go trial data in the other three conditions (75%, 50%, and 25% Go trials). As shown in Figure 7a, scalp topographical maps of target stimuli were obtained within an 800 ms time window, revealing prominent signal variations at approximately 300 ms to 400 ms at central locations among the different proportion conditions. As the proportion of Go trials

decreased, the scalp voltage in the No-Go trials decreased accordingly. We next extracted data from the average of Cz, C1, C2, FCz, FC1, FC2, PCz, PC1 and PC2 to generate waveform plots, as depicted in Figure 7b. Repeated-measures ANOVA was conducted on the amplitude of the NoGo-P3 component, indicating a significant main effect of amplitude among the three proportion conditions (F (1.305, 27.406) = 37.113, p < 0.001, η_p^2 = 0.639). In addition, repeated-measures ANOVA was conducted on the latency, which also showed a significant main effect among different proportions of Go and No-Go trials (F (1.345, 28.243) = 7.537, p = 0.006, η_p^2 = 0.264).

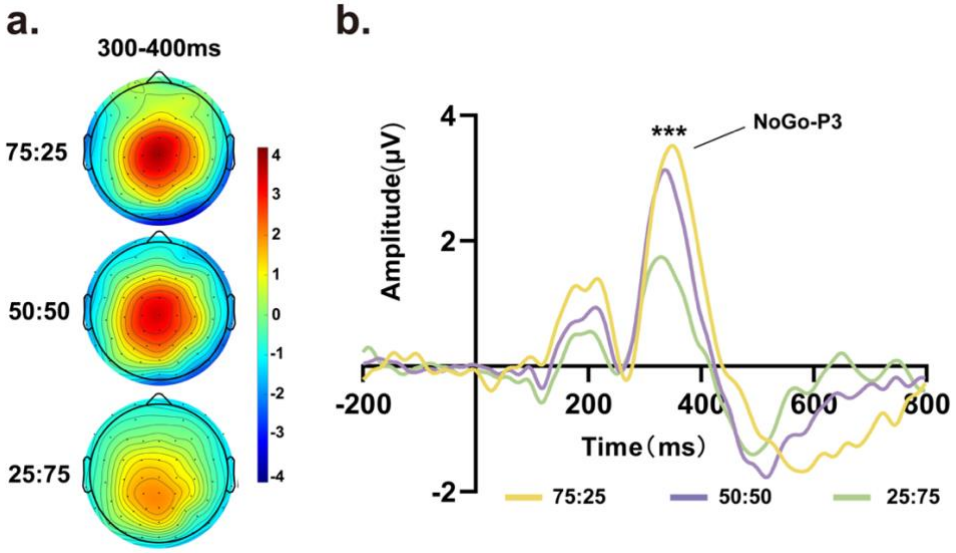

Figure 7. (a) Scalp topographic maps and waveform graphs of the average of the central electrodes (Cz, C1, C2, FCz, FC1, FC2, PCz, PC1, PC2) from 300 ms to 400 ms. In the scalp topographic map, variations in the central area can be observed under different Go and No-Go ratio conditions, with lower Go trial proportions associated with lower amplitudes. (b) Target-related ERPs of the average central electrodes, with a time window of 0-800 ms. Significant differences in the amplitude of the NoGo-P3 component were observed under different conditions. (***p < 0.001).

Furthermore, pairwise comparisons between any two conditions revealed statistically significant differences in both the amplitude and latency of the NoGo-P3 component. In particular, as shown in Figure 8a, the amplitude in the 75% Go condition was higher than those in the 50% (t (21) = 2.787, p = 0.011, d = 0.594) and 25% conditions (t (21) = 6.801, p<0.001, d = 1.450), and the second highest amplitude, which was observed in the 50% condition, was significantly higher than the amplitude in the 25% condition (t (21) = 2.104, p<0.001, d = 2.104). In addition, as shown in Figure 8b, there was no difference in the latency of the NoGo-P3 component between the 50% and 25% conditions. However, in the 75% condition, the average peak occurred later than those in the 50% and 25% conditions, and these times were significantly different (75% vs. 50%: t (21) = 4.219, p < 0.001, d = 0.900, 75% vs. 25%: t (21) = 2.812, p = 0.010, d = 0.599).

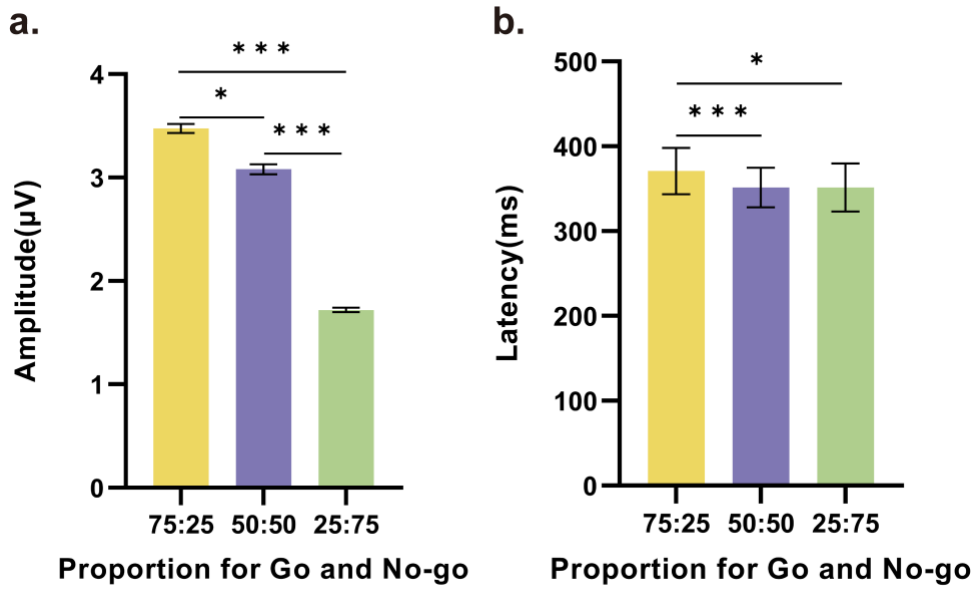

Figure 8. Significant differences in the (a) amplitude and (b) latency of the NoGo-P3 component based on the average of the central electrodes among the three conditions. Statistically significant differences were observed for nearly all comparisons between any two conditions, except for the latency between 50% and 25% (*p < 0.05, **p < 0.01, ***p < 0.001).

3.3. Discussion

In this study, we explored the effects of the ratio of Go and No-Go trials on response inhibition. The results revealed that reaction times significantly increased as the proportion of Go trials decreased. Furthermore, the error rate in the No-Go trials gradually decreased, approaching zero in the 25% Go trial condition. The ERP results also supported our hypothesis; specifically, significant differences were observed in the amplitude and latency of the NoGo-P3 component based on the average of the central electrodes (Cz, C1, C2, FCz, FC1, FC2, PCz, PC1, and PC2) under different conditions. As the proportion of Go trials decreased, the amplitude and latency of the NoGo-P3 component also gradually decreased. These findings indicate that the ratio of Go to No-Go trials affects the efficiency and capability of response inhibition.

During Go/No-Go tasks, different ratio conditions serve as prior information for participants when predicting their responses. Initially, participants compare the directions of the cue and target during the experiment. Previous studies suggest that, during this process, the brain's working memory mechanism is used to memorize and compare information [106], [107]. In the Go condition, participants push the joystick toward the response direction, while response inhibition occurs in the No-Go condition. In the 100% Go trial condition, participants only need to differentiate and remember the response direction, leading to the fastest decision-making and action execution processes. However, as the proportion of Go trials decreases, more attention is required to distinguish between trial types, resulting in slower processing speeds and increased reaction times in Go trials. Concurrently, the brain forms expectations based

on the ratio of information about upcoming target stimuli, transitioning from expecting response inhibition in the No-Go condition to expecting a response in the Go condition. Our findings are consistent with Gavazzi et al.'s recent study, which analyzed average reaction times to Go stimuli from 68 Go/No-Go studies and established a model reflecting the demand level of inhibitory control mechanisms [108]. This model used the Average Likelihood Estimation (ALE) meta-analysis algorithm and ES-SDM meta-regression to employ the mean and standard deviation of sample reaction times as linear predictor factors in three meta-regression models. The results revealed a negative correlation between average reaction time and activation in the right frontal lobe [109]. These findings suggest that assessing Go reaction times as indicators of involvement in the inhibition process enhances our understanding of the neural correlates of cognitive control for achieving inhibition. The variation in reaction times under Go conditions effectively explains the differences in the level of response inhibition influenced by expectancy. The error rate in the No-Go trials reflects participants' control over response inhibition [110], [111]. As the proportion of No-Go trials increased, the error rate decreased, indicating enhanced attention and inhibition abilities during information processing. This enhancement is related not only to adjustments after errors occur but also to expectations based on ratio information.

The electrodes in the central region, including Cz, C1, C2, FCz, FC1, FC2, PCz, PC1, and PC2, capture the NoGo-P3 component, effectively assessing the impact of different ratio conditions on response inhibition in Go/No-Go tasks. The central region typically encompasses areas such as the parietal lobe, frontal lobe, primary sensory cortex, and motor

cortex [112], [113], [114]. Electrodes placed in these areas can detect activities related to motor control and cognitive functions with high temporal precision, providing valuable insights into the neural activities underlying cognitive processing mechanisms and response inhibition [115], [116]. A larger NoGo-P3 amplitude is often interpreted as indicative of stronger response inhibition capability, while a shorter latency may suggest faster response inhibition [117], [118]. Topographical maps generated between 300 ms and 400 ms after presenting the target stimulus indicate that the primary site for processing information related to NoGo-P3 is near the central region, and the amplitude of this component decreased as the proportion of No-Go trials increased. Additionally, the waveforms show that as the proportion of No-Go trials increased, both the amplitude and latency of the NoGo-P3 component significantly decreased at the average electrode in the central region. This suggests a reduction in response inhibition capability, accompanied by an increase in the speed of response inhibition. Several studies support these findings. Albert et al. found that the NoGo-P3 component in the central region under infrequent No-Go conditions is effective for measuring brain activity related to response inhibition [119]. Smith et al. discovered that the NoGo-P3 effect is associated with cognitive or non-motor inhibition [114]. Gajewski et al.'s research linked the NoGo-P3 to inhibiting motor responses [120]. However, to our knowledge, few studies have used ERP techniques to assess the impact of different ratios of Go and No-Go stimuli on response inhibition. Different stimulus ratios trigger processes related to the brain's motor planning and prediction, which are crucial for regulating both the ability and speed of inhibitory response actions. These processes involve several functional brain areas, such as M1, PMC, and SMA, concentrated in the central region of the brain. Our results validate the

credibility of our hypothesis, demonstrating that the NoGo-P3 component in the central region can effectively assess the impact of trial ratio conditions on response inhibition in Go/No-Go tasks.

In Go/No-Go tasks, the ratio of Go to No-Go trials can influence the levels of response inhibition, potentially related to the brain's predictive mechanisms. Both prediction and response inhibition involve control, and predictive abilities may impact the effectiveness of response inhibition [105]. The brain forms expectations by recognizing stimuli and learning from prior experiences, then adjusts its responses accordingly. When external stimuli align with these expectations, the predictive mechanism enhances relevant responses, facilitating effective behavioral execution [121]. The Bayesian brain model describes this predictive mechanism, suggesting that humans use Bayesian-like reasoning when processing uncertain information, continuously updating their knowledge based on prior information and new experiences [122], [123]. Consequently, the brain adjusts its responses based on this prior information [124], [125]. In Go/No-Go tasks, the ratio of Go to No-Go trials serves as prior information, representing initial estimates of the occurrence of different types of stimuli and activating this predictive mechanism [126]. When the probability of Go stimuli is higher, participants may be more inclined to anticipate the next stimulus as a Go stimulus, making it easier to respond accordingly. Conversely, when the probability of No-Go stimuli is higher, inhibiting responses becomes easier. Therefore, varying ratios of Go and No-Go trials can affect participants' abilities to predict stimuli and inhibit responses, thereby influencing cognitive control and executive function.

3.4. Conclusion

In summary, this study suggests that different ratios of Go and No-Go trials in Go/No-Go tasks modulate response inhibition. The brain adjusts both inhibition capability and the processing rate of inhibitory responses based on this ratio information, which serves as prior knowledge. This modulation of response inhibition by trial ratios can be observed through changes in the amplitude and latency of the NoGo-P3 component recorded at electrodes in the central region (Cz, C1, C2, FCz, FC1, FC2, PCz, PC1, and PC2) during Go/No-Go tasks. As the proportion of No-Go trials increases, the amplitude and latency of the NoGo-P3 component decrease, indicating reduced response inhibition capability and slower processing of information related to response inhibition. This study expands the application of the Go/No-Go paradigm and provides valuable insights into the neural mechanisms underlying response inhibition. The results suggest promising directions for future research on modulating response inhibition.

4. Complex Network Analysis

4.1. Functional brain network on EEG data

4.1.1. Volume conduction

EEG functional connectivity can be constructed in various ways, with EEG source localization being widely used. EEG source localization is a neuroimaging technique aimed at identifying the sources or locations of specific neural activities within the brain [127], [128]. By analyzing the electrical potential data obtained from an array of electrodes placed on the scalp, the sources of these potentials, i.e., neural activities within the brain, can be inferred. Although EEG source localization is extensively used in neuroscience research, it also presents several major limitations and challenges. EEG's spatial resolution is relatively low, typically on the order of several centimeters. This means that accurately determining the specific source locations of neural activity can be challenging, especially when the sources are deep within the brain or when multiple sources are in close proximity, which limits the precision of localization [129], [130].

Volume conduction refers to the process by which electrical signals propagate from neurons inside the brain to the surface of the scalp. This process can lead to signal distortion or attenuation due to the presence of tissues such as the skull and cerebrospinal fluid [131], [132]. These tissues dampen and filter the propagation of electrical signals, causing potential deviations between the inferred signal sources from scalp electrode measurements and the actual neural source locations. To address issues related to volume conduction, researchers typically employ complex computational models, such as head models and volume

conduction models, to estimate as accurately as possible the pathways and effects of electrical signal propagation through the skull and brain tissues. Additionally, combining EEG with other brain imaging techniques, such as fMRI and MEG, can provide more comprehensive and precise localization of neural activities.

4.1.2. Phase lag index (PLI)

Phase Lag Index (PLI) is a method for detecting asymmetry in the distribution of phase differences between two signals. It reflects the consistency of whether one signal leads or lags relative to another signal and serves as an effective estimator of phase synchronization. PLI's major advantage lies in its insensitivity to volume conduction effects of the signals, focusing solely on their coupling relationships. Rosenblum et al. introduced a method for computing coupling between time series based on the concept of phase synchronization in the study of chaotic oscillators. This method does not require analyzing zero-lag synchronization, thus coupling between time series can be assessed without relying on the same source.

The specific calculation process is that if φ_1 and φ_2 are the phases of two time series, and φ is their phase difference or relative phase, then the phase synchronization index between n and m (where n and m is an integer) is defined by the following Formula 1:

$$\left|\varphi_{n,m}\right| = |n\varphi_1 + m\varphi_2| < const \quad (1)$$

This study limits m = n = 1. To calculate phase synchronization, it is necessary to know the instantaneous phase of the two signals. This can be achieved through the analytic signal and the Hilbert transform. The analytic signal $\psi(t)$ can be obtained from the real-time series $S(t)$ and the Hilbert transform of the real signal $\hat{S}(t)$, as shown in Formula 2:

$$\psi(t) = S(t) + i\tilde{S}(t) = A(t)e^{i\varphi(t)} \quad (2)$$

The Hilbert transform of $S(t)$ can be obtained through Formula 3:

$$\hat{S}(t) = \pi^{-1}P.V.\int_{-\infty}^{\infty}\frac{S(\tau)}{t-\tau}d\tau \quad (3)$$

Here, $P.V.$refers to the Cauchy principal value. After the Hilbert transform, the power spectrum of the original signal in the frequency domain remains unchanged, but the phase will experience a shift of $1/2\,\pi$. The Hilbert transform can be obtained by computing the FFT, shifting all phases by $1/2\,\pi$, and then performing the inverse FFT. Through Formula 2, both the instantaneous amplitude and instantaneous phase can be obtained. The phase $\phi(t)$ at time t can be obtained through Formula 4:

$$\phi(t) = arctan\frac{\tilde{S}(t)}{S(t)} \quad (4)$$

Through Formula 1, the phase difference or relative phase at each sampling time can be calculated from the instantaneous phases of the two signals. Subsequently, various methods have been developed to determine whether the phase difference is bounded for the convenience of calculating using the phase difference between the two signals in $\phi(t)$.

PLI estimates phase synchronization that is insensitive to common sources (such as volume conductor effects or active references) by calculating the asymmetry of the phase difference distribution, which manifests as a phase difference from 0. When there is no phase coupling relationship between the two time-series, this distribution is flat. Any deviation from this flat distribution indicates phase synchronization. The asymmetry of the phase difference distribution means that the synchronization of phase difference ϕ in $-\pi < \phi < 0$ is different from its synchronization in $0< \phi < \pi$. This asymmetry indicates a persistent, non-

zero phase difference between the two-time series, i.e., phase lag. The presence of such a phase difference and time lag cannot be explained by the influence of a single strong source or an active reference, as these influences are instantaneous. The distribution pattern is considered symmetrical when the following conditions are met: 1. When its distribution is flat (i.e., no coupling relationship exists); 2. When the phase difference is equal to or close to 0 mod π (from a strong common source or active reference).

Only in the second case, the value of phase synchronization is high while the value of the phase lag index is low. The asymmetry index of the phase difference distribution can be obtained from a time series of phase differences $\phi(t)$, t = 1… N as shown in Formula 5:

$$PLI = |\langle sing(\varphi_t)\rangle| \quad (5)$$

Here, sign denotes the sign function. Assuming: $-\pi <= \phi <= +\pi$, then the range of PLI is from 0 to 1, denoted as $0 <= PLI <= 1$. PLI equal to 0 indicates no coupling relationship or close to 0 mod π in phase difference. PLI equal to 1 indicates perfect phase locking at ϕ different from 0 mod π. The stronger the non-zero phase locking, the closer PLI approaches 1.

There is evidence suggesting that PLI performs as well as synchrony likelihood in detecting real changes in synchronization, but PLI is less influenced by signals from the same source. Besides computing global PLI, averaging PLI is also a good method to obtain local properties. In Stam's study, MEG signals were divided into five regions: frontal, temporal, central, parietal, and occipital lobes. Calculating the average PLI within each region or

between two regions proved effective as an analytical method for MEG signals.

4.1.3. Brain network construction

Based on the data collected from the ERP experiment in Chapter 3, this study constructed EEG brain networks for the No-Go task under different proportion conditions in the α (8-13 Hz), β (14-30 Hz), and θ (4-7 Hz) frequency bands. Sixty-four scalp electrodes were used as network nodes, and the phase lag index, which can better mitigate the volume conduction effect, was used as the measure of connection strength between nodes. The functional connectivity networks, after calculation, are shown in Figure 9.

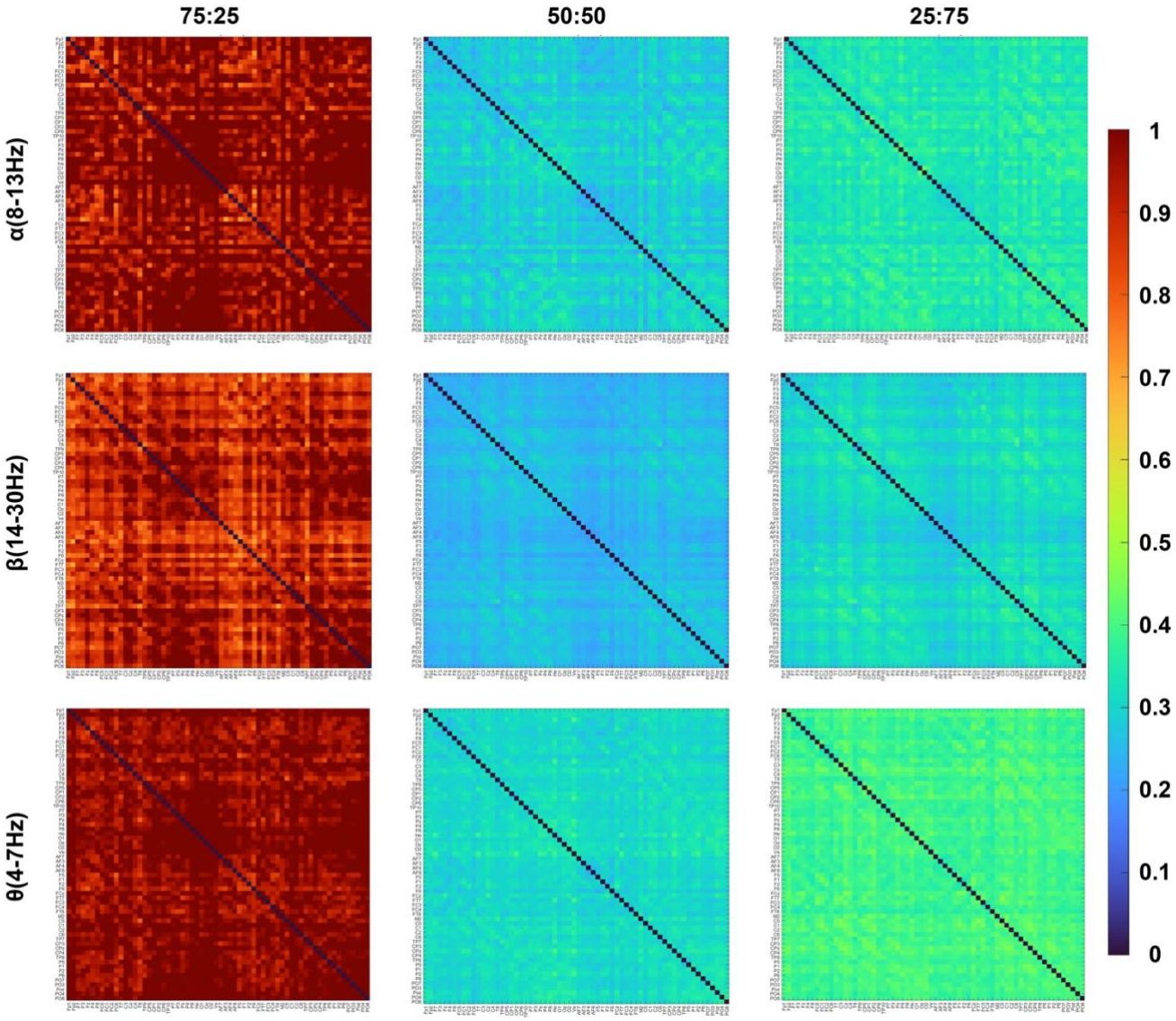

Figure 9. The functional networks constructed for different Go and No-Go ratio conditions across different frequency bands. Red indicates that the PLV is close to 1, representing a strong coupling relationship and stronger functional connectivity. Blue indicates that the PLV is close to 0, representing no coupling relationship and weaker functional connectivity. The labels on the horizontal and vertical axes of each matrix, from top to bottom (left to right), are as follows: Fp1, Fp2, F7, F3, Fz, F4, F8, FC5, FC1, FC2, FC6, T7, C3, Cz, C4, T8, TP9, CP5, CP1, CP2, TP10, P7, P3, Pz, P4, P8, He, O1, Oz, O2, Ve, AF7, AF3, AF4, AF8, F5, F1, F2, F6, FCz, FT7, FC3, FC4, FT8, M2, C5, C1, C2, C2, C6, TP7, CP3, CPz, CP4, TP8, P5, P1, P2, P6, PO7, PO3, POz, PO4, PO8.

4.2. Network properties

4.2.1. Clustering coefficient

This reflects the subgroup structure and network clustering of the nodes. The higher the clustering coefficient, the more closely the nodes around a given node are connected to each other. The clustering coefficient is calculated based on the ratio of the number of actual connections between nodes to the maximum possible number of connections. The overall clustering coefficient is defined in terms of closed triplets (triangles). If a part of the graph has nodes that are pairwise connected, many "triangles" can be identified, where the three points are pairwise connected, forming a closed triplet. Additionally, there are open triplets, where three points are connected by two edges (a triangle missing one edge). These two types of triplets constitute all connected triplets. The overall clustering coefficient is defined as the ratio of the number of closed triplets to the total number of connected triplets (both open and closed) in the graph.

The clustering coefficient can measure the clustering characteristics and tightness within the brain functional network, reflecting the likelihood that the neighboring nodes of a certain node in the network are also neighbors with each other. For instance, the clustering coefficient of node i in the network is defined as the ratio of the actual number of edges E_i existing among the neighboring nodes connected to node i to the maximum possible number of edges among the neighboring nodes, as shown in Formula 6:

$$C_i = \frac{2E_i}{k_i(k_i-1)} \tag{6}$$

Here, k_i represents the number of neighboring nodes of that node, and $k_i(k_i-1)/2$ represents the maximum possible number of edges among these k_i neighboring nodes. Due to the large number of nodes in a complex network, the clustering coefficient of each node in the brain network is not studied; instead, the average clustering coefficient of the entire network is analyzed. In an unweighted network, the average clustering coefficient C_i of the network is the average of the clustering coefficients of all nodes, reflecting the clustering connections around a single node, as shown in Formula 7:

$$C_i = \frac{1}{N}\sum_{i=1}^{N} C_i \tag{7}$$

4.2.2. Characteristic path length

A key indicator of information integration efficiency between brain regions is the characteristic path length. The calculation of characteristic path length involves determining the shortest path lengths between all pairs of nodes in the network. In a network, the shortest path between two nodes is the path with the fewest edges connecting those nodes. The characteristic path length is the average of all such shortest path lengths. In network analysis, a smaller characteristic path length indicates faster information transmission speed in the

network, signifying higher network efficiency.

In complex networks, different nodes can be connected through different paths, and these paths are called edges. The number of edges traversed is called the path length. For example, from node i to node j, the number of edges that need to be traversed is the path length. There are many choices for this path, but there exists a path with the shortest length, called the optimal path, which can transmit information from node i to node j. The number of edges on this shortest path is the shortest path length between these two nodes. The average of the shortest path lengths between any two nodes is defined as the characteristic path length L, which describes the network's internal information transmission capability and reflects the strength of functional integration between brain regions. The shorter the path length, the greater the strength of functional integration, indicating more direct connections between brain regions. The definition of characteristic path length can be expressed as Formula 8:

$$L = \frac{\sum_{i \geq j} L_{ij}}{\frac{1}{2}N(N+1)} \tag{8}$$

Where L_{ij} is the shortest path length between node i and node j, and N is the number of nodes.

4.2.3. Global efficiency

It is the average of the reciprocals of the shortest path lengths in the network. Global efficiency is considered a good indicator of the information processing efficiency of brain functional networks. High global efficiency means that information in the brain can be transmitted efficiently through shorter paths, which is often associated with better cognitive

abilities.

Global efficiency is the average of the inverses of the shortest path lengths and can be used to measure the efficiency of the brain functional network in transmitting and processing information. Additionally, it is commonly used in networks with disconnected nodes. The presence of disconnected nodes may result in infinite values when calculating the shortest path length between such nodes and others, affecting the computation of the characteristic path length. Since global efficiency allows for the presence of isolated nodes, using global efficiency provides a more comprehensive description of brain network characteristics, especially in non-connected networks. The definition of global efficiency E_g is shown in Formula 9:

$$E_g = \frac{1}{N(N-1)} \sum_{i \neq j} \frac{1}{L_{ij}} \tag{9}$$

Both characteristic path length and global efficiency are metrics that can effectively measure the global information processing and transmission capability of the network, as well as the degree of network integration.

4.2.4. Local efficiency

The average global efficiency of the subgraph formed by the neighbors of a given node. Local efficiency for a network is the average of the local efficiencies of all nodes in the network. Global efficiency and mean path length indicate the integration of brain networks. Local efficiency, clustering coefficient, and centrality provide information about the segregation of network activities.

Local efficiency can also measure the degree of differentiation in the network, with the calculation shown as Formula 10:

$$E_{loc} = \frac{1}{N}\sum_{i\in G} E_g \tag{10}$$

In the process of information flow processing, the brain primarily involves closely related and coordinated brain regions, leading to the clustering characteristics of functional differentiation among the involved brain regions. The clustering coefficient C_i and local efficiency E_{loc} can effectively measure the local characteristics of brain networks and contribute to information processing in the brain.

4.2.5. Node degree

Among all centrality measures, degree is the most basic and important metric in a network. The degree of a node indicates the total number of edges associated with that node, i.e., the number of edges passing through that node, which is also equal to the number of neighboring nodes the node has. The larger the degree value of a node, the more important the node is in the network. The degree of node i can be defined by Formula 11:

$$D_i = \sum_{j=1}^{N} a_{ij} \tag{11}$$

Where a_{ij} is an element of the binary network, the number of nodes, i.e., the network size, is N. a_{ij} is 0 if node i and node j are not connected, and a_{ij} is 1 if node i and node j are connected. The average degree of nodes in the network is defined as the average of the degrees of all N nodes, as shown in Formula 12:

$$\langle D\rangle = \frac{1}{N}\sum_i D_i \tag{12}$$

The average degree of nodes can reflect the sparsity of edges in the network. For directed graphs, the degree of a node is divided into two types: in-degree D_i^{in} and out-degree D_i^{out},

which correspond to the number of edges pointing to the node (in-degree) and the number of edges the node points to other nodes (out-degree), respectively. For node i the definitions of D_i^{in} and D_i^{out} are shown in Formulas 13 and 14, respectively:

$$D_i^{in} = \sum_i a_{ij} \tag{13}$$

$$D_i^{out} = \sum_i a_{ji} \tag{14}$$

Among them, $D_i = D_i^{in} + D_i^{out}$, where the average values of out-degree and in-degree are the same, as shown in Formula 15:

$$\langle D_i^{in} \rangle = \langle D_i^{out} \rangle = \frac{1}{N} \sum_{ij} a_{ji} \tag{15}$$

4.2.6. Node betweenness centrality

Another important node attribute is betweenness, which reflects the importance of a node or edge in a network. It represents the number of shortest paths that pass through a particular node or edge. In information exchange, a node with higher betweenness indicates that there are more shortest paths passing through it, and thus, it handles more information. Betweenness centrality refers to the proportion of the shortest paths in the network that pass through a particular node, and it characterizes the centrality of that node. A higher betweenness centrality means that the node carries more information flow and has a greater impact on the performance of the functional brain network. In unweighted brain networks, the definition of betweenness centrality is given by Formula 16:

$$C_B(i) = \frac{2 \sum_{h<j \in V} g_{hj}(i)}{\substack{h \neq i, j \neq i \\ (N-1)(N-2) g_{hj}}} \tag{16}$$

Here, g_{hj} is the number of all shortest paths between node $h \in V$ and node $j \in V$, where V is the set of all nodes in the network. $g_{hj}(i)$ represents the number of all shortest paths

from node $h \in V$ to node $j \in V$ that passthrough node i.

4.3. Results

4.3.1. Global measures

This study conducted a complex network analysis of functional connectivity in ERP data from No-Go tasks with different proportions of Go and No-Go trials. The experimental conditions included ratios of 75:25, 50:50, and 25:75 for Go and No-Go trials. Functional connectivity was assessed using the phase lag index (PLI) and analyzed in the α, β, and θ frequency bands. We calculated four global network properties—clustering coefficient, characteristic path length, global efficiency, and local efficiency—as well as two local properties—node degree and betweenness centrality. Statistical analysis of the differences in network properties under varying ratio conditions across frequency bands was performed using repeated measures ANOVA, with Bonferroni correction applied.

The results, as shown in Figure 10, indicate that in the α frequency band, statistical differences were observed only in the global properties of Global Efficiency and Characteristic Path Length. Specifically, as the proportion of Go trials decreased, Global Efficiency exhibited a decreasing trend, while Characteristic Path Length showed an increasing trend. Global Efficiency demonstrated statistically significant differences between the 75% Go condition and the other two conditions ($p < 0.05$). For Characteristic Path Length, statistically significant differences were found only between the 75% and 25% Go conditions.

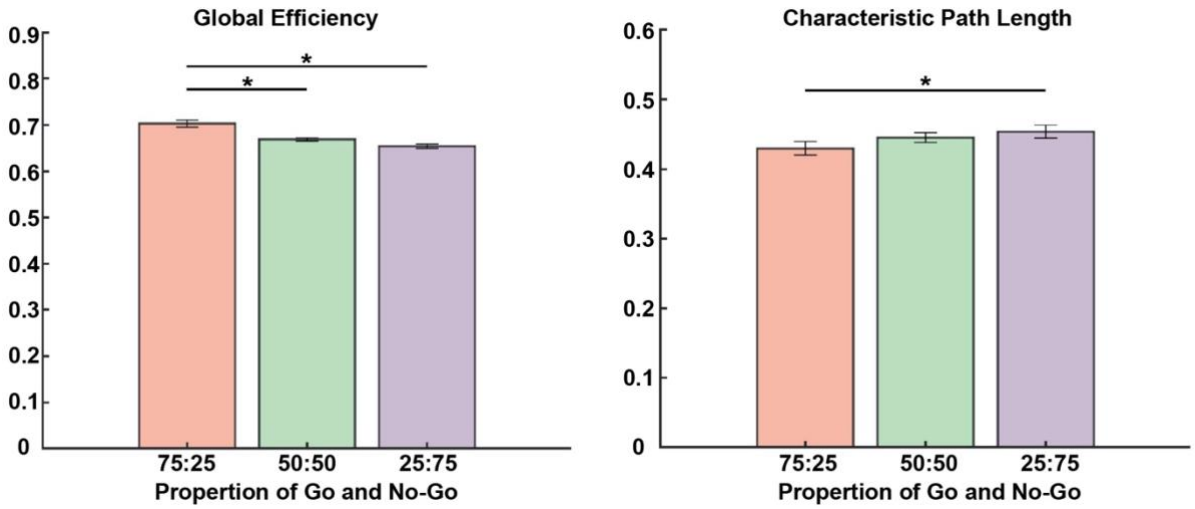

Figure 10. Differences in global properties under conditions with different proportions of Go trials in the α frequency band. As the proportion of Go trials decreases, Global Efficiency shows a decreasing trend, while Characteristic Path Length shows an increasing trend.

The results for the β frequency band, as shown in Figure 11, indicate that all four global properties exhibited statistical differences. Specifically, as the proportion of Go trials decreased, Global Efficiency, Local Efficiency, and Clustering Coefficient showed decreasing trends, while Characteristic Path Length showed an increasing trend. Local Efficiency and Global Efficiency demonstrated statistically significant differences between the 75% Go condition and the other two conditions. The Clustering Coefficient and Characteristic Path Length exhibited statistically significant differences between all pairs of conditions ($p < 0.05$).

Figure 12 shows the results of global properties for different Go trial conditions in the θ frequency band. The results indicate that all four global properties exhibited statistical differences. Specifically, as the proportion of Go trials decreased, Global Efficiency, Local Efficiency, and Clustering Coefficient showed decreasing trends, while Characteristic Path

Length showed an increasing trend, consistent with findings from the other two frequency bands. Local Efficiency and Clustering Coefficient showed statistically significant differences between the 75% Go condition and the 25% Go condition. Global Efficiency and Characteristic Path Length exhibited statistically significant differences between the 75% Go condition and the other two conditions ($p < 0.05$).

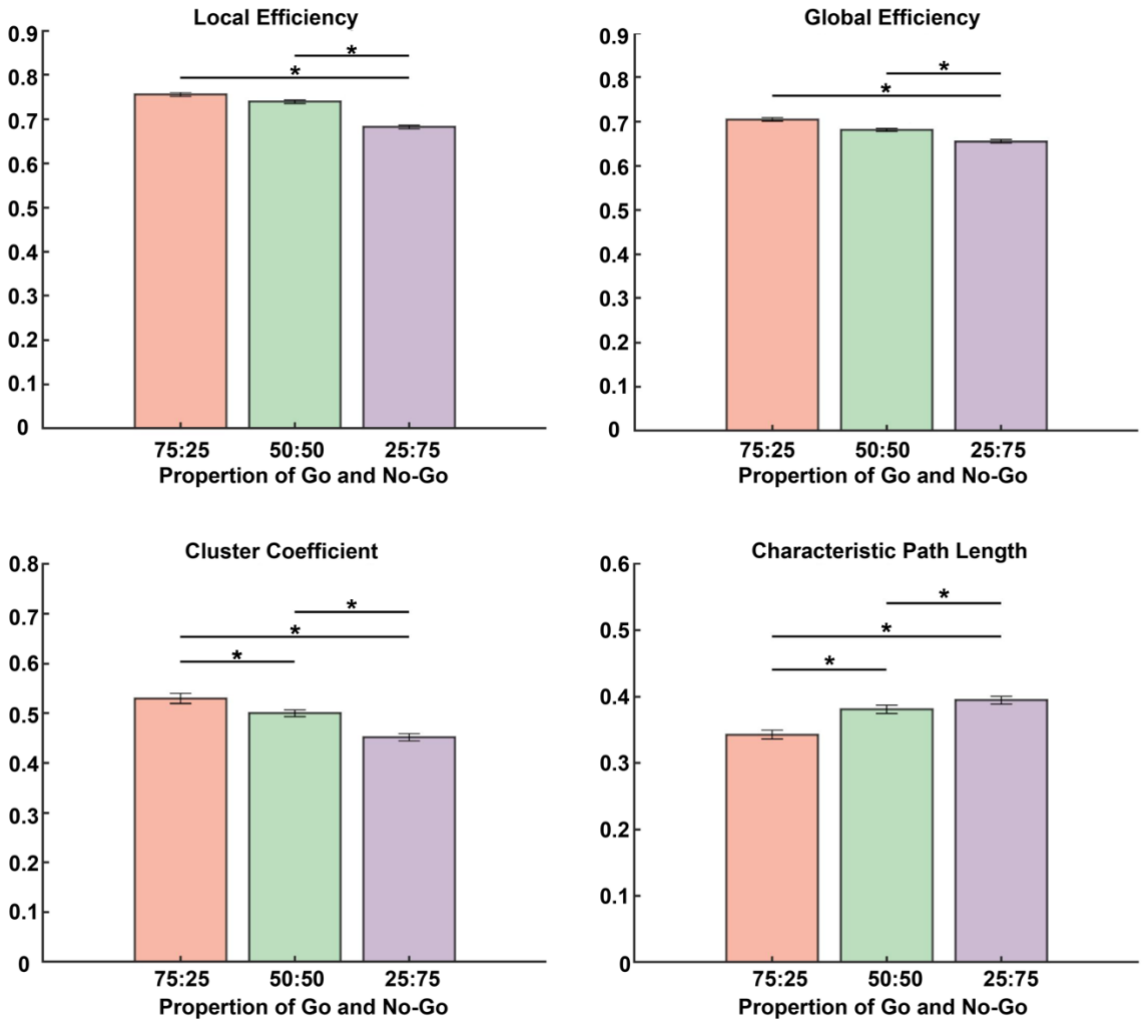

Figure 11. Differences in global properties under conditions with different proportions of Go trials in the β frequency band. As the proportion of Go trials decreased, Global Efficiency, Local Efficiency, and Clustering Coefficient showed decreasing trends, while Characteristic Path Length showed an increasing trend.

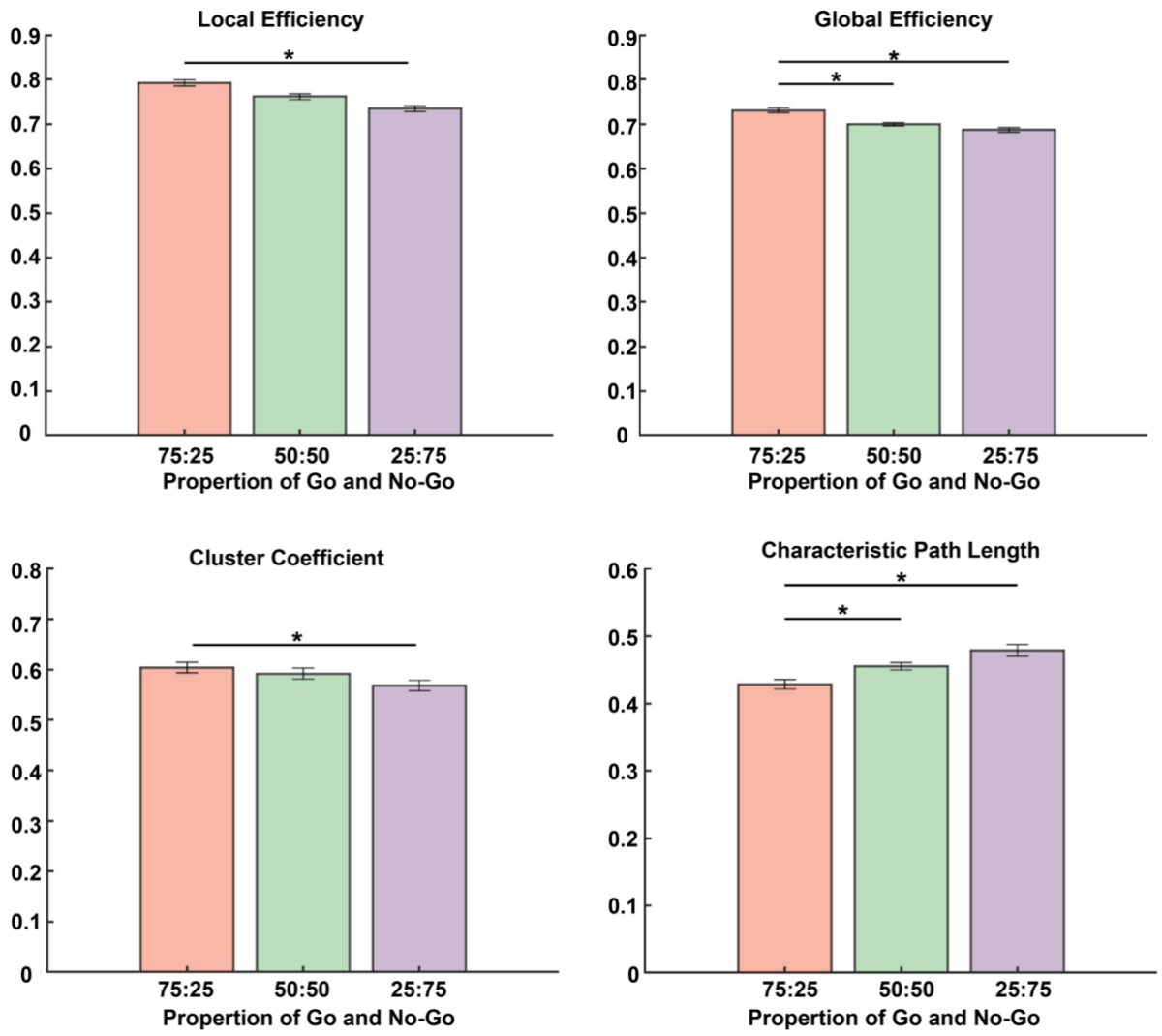

Figure 12. Differences in global properties under conditions with different proportions of Go trials in the θ frequency band. As the proportion of Go trials decreased, Global Efficiency, Local Efficiency, and Clustering Coefficient showed decreasing trends, while Characteristic Path Length showed an increasing trend.

4.3.2. Local measures

Statistical differences in betweenness centrality and node degree under different proportion conditions across various frequency bands are recorded in Table 1 (betweenness centrality) and Table 2 (node degree). The results show that electrode nodes with significant differences in these attributes are predominantly distributed in the frontal lobe, central area, and parietal

lobe. Moreover, as the number of Go trials decreases, both betweenness centrality and node degree exhibit a statistically significant decrease. Additionally, more electrodes showed significant differences in the β and θ frequency bands compared to the α frequency band.

Table 1. Differences in betweenness centrality under conditions with different proportions of Go trials.

Band	Electrode	*F* value	*p* value
α	AF7	4.684	0.015
	C5	7.193	0.002
	F7	7.069	0.002
	F8	4.491	0.017
	P2	8.414	<0.001
	P4	7.634	<0.001
	POz	4.162	0.224
β	AF3	3.899	0.025
	C1	3.736	0.032
	C2	3.469	0.042
	C3	3.894	0.028
	CP6	3.699	0.033
	F8	3.317	0.046
	FC1	5.276	0.009
	FP1	7.224	0.002
	FP2	6.537	0.003

	P3	3.936	0.027
θ	AF4	5.522	0.007
	AF7	3.616	0.035
	AF8	5.166	0.009
	C1	5.397	0.008
	CP2	3.494	0.036
	CPz	4.139	0.022
	Cz	3.381	0.043
	F4	3.781	0.031
	FC5	4.459	0.018
	P4	3.603	0.036
	P6	5.238	0.009
	P8	4.163	0.022
	PO4	4.501	0.015
	PO8	3.906	0.028

Table 2. Differences in node degree under conditions with different proportions of Go trials.

Band	Electrode	*F* value	*p* value
α	AF7	3.683	0.034
	C5	8.085	0.001
	CP5	6.382	0.004
	F7	3.752	0.032

	F8	4.877	0.012
	FC3	4.033	0.025
	FC5	3.984	0.026
	P2	7.695	0.001
	P4	4.909	0.012
	PO4	8.502	<0.001
	POz	3.875	0.028
β	AF3	4.428	0.018
	AF4	7.445	0.001
	AF7	5.061	0.011
	C5	4.240	0.021
	CP2	4.669	0.015
	CP3	5.959	0.005
	F2	7.342	0.002
	F4	11.588	<0.001
	F5	7.671	0.001
	F6	4.665	0.015
	F7	4.373	0.019
	F8	4.509	0.017
	FC1	4.450	0.018
	FP1	7.311	0.002
	FP2	11.067	<0.001

	P2	4.232	0.021
	P3	6.413	0.004
	PO8	5.528	0.008
	Pz	4.995	0.011
θ	AF4	5.742	0.006
	C1	6.881	0.002
	C4	5.877	0.006
	C5	4.559	0.016
	CP2	5.808	0.006
	CP4	3.926	0.027
	CPz	12.760	<0.001
	Cz	6.904	0.003
	F4	3.478	0.040
	F5	5.369	0.008
	FC2	3.344	0.044
	FC5	6.979	0.002
	P1	3.297	0.046
	P2	6.126	0.005
	P4	3.721	0.032
	P6	3.589	0.036
	P8	4.256	0.021
	PO4	3.806	0.030

	POz	4.278	0.021
	Pz	4.707	0.014

4.4. Discussion

Chapters 2 and 3 have shown that in Go/No-Go tasks, different ratios of Go and No-Go trials modulate response inhibition. The brain adjusts its inhibition capability and the processing speed of inhibitory responses based on this ratio information. This modulation of response inhibition due to trial ratios can be observed through changes in the amplitude and latency of the NoGo-P3 component recorded at electrodes in the central region during Go/No-Go tasks. As the proportion of No-Go trials increases, the amplitude and latency of the NoGo-P3 component decrease, indicating a reduction in response inhibition capability and a slower processing speed of information related to response inhibition. Building on these findings, the present chapter constructs EEG functional brain networks for No-Go trials and performs a network property analysis. Unlike traditional time-domain and frequency-domain analyses, which interpret results using single-dimensional information, this method employs dynamic time-frequency analysis to examine the influence of different trial ratios on response inhibition capability from a whole-brain perspective.

As the number of Go trials decreases, the increase in reaction time and the changes in the amplitude and latency of the NoGo-P3 component indirectly reflect a reduction in response inhibition capability and a slower processing rate of information involved in response inhibition. These changes can be explained through the global properties of the network. Higher global

efficiency indicates that information transfer across the entire network becomes more efficient [133], [134]. As the number of No-Go trials increases, response inhibition ability gradually weakens, and the information processing rate in the whole-brain network decreases, which is reflected by a reduction in global efficiency. An increase in local efficiency signifies more frequent information transfer and interaction within the neighborhood of each node [135]. When the number of No-Go trials increases, the speed of response inhibition decreases, leading to reduced information exchange between nodes involved in response inhibition processing, and thus a decrease in local efficiency. An increase in characteristic path length means that the average shortest path between two nodes in the network becomes longer, resulting in slower information transfer, which is the opposite of global efficiency [136], [137]. A decrease in the clustering coefficient indicates a lower degree of node clustering in the network, making the local network structure more sparse, which is typically associated with weakened response inhibition ability [138]. Regarding local properties, node degree represents the number of other nodes directly connected to a node. When response inhibition ability improves, key nodes may connect to more other nodes, increasing their node degree. This reflects an increase in the importance of these nodes in information transfer, with more information passing through and being processed by them. Betweenness centrality measures the number of shortest paths passing through a node. When response inhibition ability improves, certain nodes may play more critical roles in the network, becoming key channels through which more information flows. This increases their betweenness centrality, reflecting their crucial role in information transfer and overall network efficiency [139], [140]. A decrease in node degree and betweenness centrality as the number of Go trials decreases indicates

that connectivity and the information exchange rate between nodes involved in response inhibition processing diminish, leading to weakened response inhibition ability and slower processing speed.

In the study of response inhibition, brain activity in different frequency bands serves distinct functional roles and provides information about various neural processing mechanisms [141], [142]. Our results show that electrodes with differential nodal properties in the θ and β bands are more numerous than those in the α band. The α band is typically associated with resting states, background inhibitory control, and passive information processing [143]. In response inhibition tasks, α band activity more prominently reflects the brain's ability to inhibit irrelevant information or interference. Since the α band primarily involves overall inhibitory mechanisms and background processing, it plays a more global, holistic inhibitory role rather than showing specific nodal differences. In response inhibition tasks, α band activity more prominently reflects the brain's ability to inhibit irrelevant information or interference. Since the α band primarily involves overall inhibitory mechanisms and background processing, it plays a more global, holistic inhibitory role rather than showing specific nodal differences. β band activity is associated with motor control, planning, and execution [144]. In response inhibition tasks, a decrease in β band activity usually indicates the inhibition of motor responses. This involves precise coordination among specific brain regions (such as the primary motor cortex and the prefrontal cortex). Therefore, the β band shows more information processing and nodal activity during response inhibition, reflecting the coordinated work of different brain regions in inhibiting motor responses. The α band has the fewest nodes with differential network

properties, while the θ and β bands have more. This reflects the different emphases and levels of information processing in the brain across various frequency bands. The α band primarily reflects global inhibitory control, whereas the θ and β bands reflect the dynamic coordination and information exchange among specific brain regions during complex cognitive tasks and motor control.

Response inhibition is a complex and critical executive function involving the coordination of multiple brain networks and regions. The prefrontal cortex, particularly the dorsolateral prefrontal cortex (DLPFC) and ventrolateral prefrontal cortex (VLPFC), plays a central role in this process [145], [146], [147]. The DLPFC is associated with working memory and executive control, helping to manage and inhibit unnecessary responses, while the VLPFC is crucial for inhibiting specific responses and handling conflicts. The parietal cortex, involved in integrating attention and perception, collaborates with the prefrontal cortex to adjust and maintain attention during selective attention and response inhibition processes. The central executive network (CEN), which includes the DLPFC and posterior parietal cortex (PPC), is responsible for higher-level cognitive functions such as decision-making and control, coordinating other networks to ensure appropriate responses are selected and executed during response inhibition [148]. The DLPFC is associated with working memory and executive control, helping to manage and inhibit unnecessary responses, while the VLPFC is crucial for inhibiting specific responses and handling conflicts. The parietal cortex, involved in integrating attention and perception, collaborates with the prefrontal cortex to adjust and maintain attention during selective attention and response inhibition processes. The central

executive network (CEN), which includes the DLPFC and posterior parietal cortex (PPC), is responsible for higher-level cognitive functions such as decision-making and control, coordinating other networks to ensure appropriate responses are selected and executed during response inhibition [149], [150], [151]. The prefrontal cortex influences motor areas via subcortical pathways, such as through the basal ganglia and thalamus, to regulate movement initiation and inhibition. The central executive network coordinates the flow of information between different cortical regions to ensure effective response inhibition. In our research, we found significant differences in node degree and betweenness centrality among nodes related to response inhibition. Node degree refers to the number of direct connections a node has with other nodes, while betweenness centrality reflects the extent to which a node acts as a mediator between other nodes in the network [152]. The results showed that key nodes in the prefrontal cortex, parietal cortex, and motor network exhibited notable differences in these metrics. Key nodes in the prefrontal cortex typically had higher node degree and betweenness centrality, indicating their crucial role in integrating and coordinating processes during response inhibition. Key nodes in the parietal cortex also demonstrated high node degree and betweenness centrality in the transmission of sensory and attentional information, while key nodes in the motor network showed elevated values in these metrics for regulating motor planning and execution. These findings further support the idea that response inhibition is the result of the collective action of multiple brain regions and networks, with the prefrontal cortex playing a central role [153], [154]. The parietal cortex provides sensory and attentional support, the motor network executes specific actions, and the central executive network coordinates the overall process. These brain regions and networks

achieve response inhibition through complex neural connections and information exchange.

4.5. Conclusion

This chapter constructs EEG functional brain networks for No-Go trials and performs network property analysis. Unlike traditional time-domain and frequency-domain analyses, which use single-dimensional information, this method employs dynamic time-frequency analysis to interpret the impact of different ratios on response inhibition from a whole-brain perspective. The study finds that as the number of Go trials decreases, increases in reaction time and changes in the amplitude and latency of the NoGo-P3 component indirectly reflect reduced and slower processing of information related to response inhibition. These changes are explained through global network properties: global efficiency decreases, local efficiency decreases, characteristic path length increases, and clustering coefficient decreases. For local properties, decreased node degree and betweenness centrality indicate reduced information exchange rates between nodes involved in response inhibition. Brain activity in different frequency bands serves distinct functions in response inhibition: α band activity is associated with overall inhibitory control; θ band activity is linked to cognitive control and task-related processes; and β band activity is related to motor control and execution. The study shows that the prefrontal cortex, parietal cortex, and motor network exhibit significant differences in node degree and betweenness centrality, highlighting their crucial roles in response inhibition. The findings support the notion that response inhibition results from the collective action of multiple brain regions and networks, with the prefrontal cortex playing a central role, the parietal cortex providing sensory and attentional support, the motor network executing specific actions, and the central executive network coordinating the overall process.

5. Conclusion and limitations

In Chapter 1, we introduce and explain several relevant concepts related to this topic, including response inhibition, the Go/No-Go task, EEG signals, and the characteristics and analysis methods of EEG, including both traditional and nonlinear approaches. We discuss the advantages and disadvantages of these analysis methods and then introduce the new analysis method used in our study—complex network analysis. Complex network analysis, based on functional connectivity, leverages the high temporal resolution of EEG while also interpreting its spatial properties. This chapter also provides a detailed explanation of graph theory and introduces various complex network metrics widely used across different fields. Based on these theories and concepts, we review the current state of research both domestically and internationally. Response inhibition refers to an individual's ability to suppress or delay their response when faced with stimuli, which is crucial in daily life and highly valuable in neuroscience research. The neural mechanisms typically involve the prefrontal cortex, the anterior cingulate gyrus, and the basal ganglia, and the Go/No-Go task is widely used to assess this ability. This task includes two types of stimuli: Go stimuli (requiring a response) and No-Go stimuli (requiring response inhibition). Reaction time serves as a genuine measure to assess the underlying psychological mechanisms. In Go/No-Go experiments, reaction time to Go stimuli reflects the efficiency of inhibition processes. Assumptions about inhibition processes have been temporally validated, and models based on reaction time help in understanding inhibition mechanisms. The relationship between reaction time and inhibition mechanisms under different ratios of Go and No-Go conditions is still being explored. Event-related potential (ERP) studies show that the prefrontal regions

play a key role in response inhibition. The P3 component (around 300 milliseconds) is used as a marker of how the brain processes stimuli. Recent studies indicate that the central P3 component associated with No-Go conditions is related to the response inhibition process. The ratio of Go and No-Go stimuli affects the predictive mechanism, thereby influencing response inhibition. Complex network analysis offers a new approach to studying dynamic functional connectivity in the brain, whereas traditional ERP analysis focuses on neural activity at specific time points.

Based on this research background, we propose the following research objectives:1. In the behavioral experiment, we set ISI and ratio as two independent variables to explore whether ISI and the Go/No-Go ratio have a statistically significant impact on Go reaction time, with ISI being a parameter in the experimental design.2.Based on the behavioral experiment, we selected a fixed ISI and analyzed ERP components to investigate the impact of different ratios on the neural mechanisms of response inhibition. We examined the reaction time in Go trials and the error rate in No-Go trials under different conditions to assess the influence of prior probability on reaction control. We also analyzed the ERP components, particularly the amplitude and latency of the NoGo-P3 component in the central region. The NoGo-P3 component effectively reflects the response inhibition process.3. Based on the ERP experiment, we conducted a complex network analysis of the collected whole-brain EEG data to explore the impact of the Go/No-Go ratio on response inhibition from the perspective of overall and dynamic characteristics of functional network connectivity.

In Chapter 2, we explored the effects of different Go and No-Go trial ratios and ISI on response inhibition in Go/No-Go experiments. The ratio of Go to No-Go trials significantly influenced the reaction times for Go trials. Specifically, as the proportion of Go trials decreased, reaction times increased. The study found no significant interaction between the ratios of Go and No-Go trials and ISI, indicating that these factors independently affect response inhibition processes. Although ISI settings did not show statistically significant effects on response inhibition in this study, different ISI intervals provided stable results in Go trial responses, particularly at intervals of 300 ms or more. Overall, these findings highlight the importance of considering ratio conditions and ISI settings when studying response inhibition and cognitive control mechanisms. They offer insights into how experimental designs can enhance our understanding of complex cognitive processes and neural dynamics in Go/No-Go tasks.

In Chapter 3, the ERP study suggests that different ratios of Go and No-Go trials in Go/No-Go tasks modulate response inhibition. The brain adjusts its inhibition capability and the processing rate of inhibitory responses based on this ratio information, which serves as prior knowledge. This modulation of response inhibition by the trial ratio can be observed through changes in the amplitude and latency of the NoGo-P3 component recorded at electrodes in the central region (Cz, C1, C2, FCz, FC1, FC2, PCz, PC1, and PC2) during Go/No-Go tasks. As the proportion of No-Go trials increases, the amplitude and latency of the NoGo-P3 component decrease, indicating reduced response inhibition capability and slower processing of information related to response inhibition. This study expands the application

of the Go/No-Go paradigm and provides crucial insights into the neural mechanisms underlying response inhibition, suggesting promising directions for future research on modulating response inhibition.

Chapter 4 constructs EEG functional brain networks for No-Go trials and performs network property analysis. Unlike traditional time-domain and frequency-domain analyses, which utilize single-dimensional information, this method employs dynamic time-frequency analysis to interpret the impact of different ratios on response inhibition from a whole-brain perspective. The study finds that as the number of Go trials decreases, increases in reaction time and changes in the amplitude and latency of the NoGo-P3 component indirectly reflect reduced and slower processing of information related to response inhibition. These changes are explained through global network properties: global efficiency decreases, local efficiency decreases, characteristic path length increases, and clustering coefficient decreases. In terms of local properties, decreased node degree and betweenness centrality indicate reduced connectivity and information exchange rates between nodes involved in response inhibition. Brain activity in different frequency bands serves distinct functions in response inhibition: α band activity is associated with overall inhibitory control; θ band activity is linked to cognitive control and task-related processes; and β band activity is related to motor control and execution. The study shows that the prefrontal cortex, parietal cortex, and motor network exhibit significant differences in node degree and betweenness centrality, highlighting their crucial roles in response inhibition. The findings support the idea that response inhibition results from the collective action of multiple brain regions and networks, with the prefrontal

cortex playing a central role, the parietal cortex providing sensory and attentional support, the motor network executing specific actions, and the central executive network coordinating the overall process.

Chapter 5 provides a summary and discusses the limitations of our study. We briefly review the findings from the previous chapters and address the limitations of our research, as well as suggest future research directions. In our behavioral experiments, we explored the effects of Go/No-Go ratios and ISI on response inhibition. However, due to constraints on experimental duration, we did not test all possible ratios, and the number of ISI conditions was also limited. Future studies could include supplementary experiments to examine a broader range of threshold conditions. In Chapter 3, we focused on the NoGo-P3 component but only analyzed the central region. Other components related to response inhibition, such as the NoGo-N2 component, and additional brain regions, like the frontal and parietal lobes, are also valuable for research. Future research could explore these components and regions in greater depth. In Chapter 4, we applied complex network analysis to EEG data based on functional connectivity. While our findings were valuable, our calculation of functional connectivity utilized PLV among other methods like effective connectivity. We chose commonly used metrics for complex network evaluation. These considerations will guide future studies in further exploring the neural mechanisms of response inhibition.

Publications

1. **Nan Zhang**, Weichao An, Yinghua Yu, Jinglong Wu, Jiajia Yang. Go/No-Go Ratios Modulate Inhibition-Related Brain Activity: An Event-Related Potential Study. *Brain Science*, 2024, 14(5): 414.
2. **Nan Zhang**, Yinghua Yu, Hiroki Yamamoto, Jinglong Wu, Yoshimichi Ejima, Hiroshi Kadota, Kiyoshi. Nakahara, Hiroaki Shigemasu, Jiajia.Yang. Different Brain Activity in Tactile Working Memory Across Varied Delay Times. The 7th Japanese meeting for Human Brain Imaging (JHBI). (Tamagawa University, Tokyo, Japan, 2023-9).
3. **Nan Zhang**, Weichao An, Yan Niu, Jiajia Yang, Yinghua Yu, Yoshimichi Ejima, Jinglong Wu. Abnormal brain network entropy of resting state fMRI in schizophrenia. The 16th International Conference on Complex Medical Engineering (ICME 2022).

Acknowledgement

First and foremost, I would like to express my heartfelt gratitude to my advisor, Professor Jiajia Yang. As someone who only began studying cognitive neuroscience during my doctoral studies, I found that both the approach to thinking about scientific questions and the methods of solving problems in this field were vastly different from what I had previously known. I am deeply grateful to Professor Yang for his professional knowledge and patience in guiding and assisting me academically, which has greatly benefited me and allowed me to complete my research tasks and graduate on time.

Secondly, I am especially thankful to Professor Jinglong Wu. It was his acceptance of me, despite my lack of a background in this field, that gave me the opportunity to travel across the ocean and experience a memorable study abroad life in Japan. For someone from an ordinary family, this was an incredibly precious opportunity. I am also grateful to Professor Wu for his constant care, which made me feel the warmth, even while I was far from home.

Additionally, I want to thank Professor Yinghua Yu from the research group, who provided me with substantial help during my studies and research. Particularly during my early days at the university, Professor Yu patiently taught me advanced MRI techniques, allowing me to gain valuable knowledge and experience. I would also like to acknowledge the support and guidance of Professor Takahashi and Professor Ejima from Kyoto University, who contributed significantly to my research.

Acknowledgement

Due to the impact of the COVID-19, I was supposed to start my studies in October 2021 but did not arrive in Japan until June of the following year. Despite my lack of professional background, I managed to graduate on time, which would not have been possible without the help of the professors and classmates in the research group. For this, I offer my most sincere thanks.

Reference

[1] E. Congdon, J. A. Mumford, J. R. Cohen, A. Galvan, T. Canli, and R. A. Poldrack, “Measurement and reliability of response inhibition,” *Front Psychol*, vol. 3, no. FEB, 2012, doi: 10.3389/fpsyg.2012.00037.

[2] F. Verbruggen and G. D. Logan, “Response inhibition in the stop-signal paradigm,” Nov. 2008. doi: 10.1016/j.tics.2008.07.005.

[3] K. R. Ridderinkhof, W. P. M. Van Den Wildenberg, S. J. Segalowitz, and C. S. Carter, “Neurocognitive mechanisms of cognitive control: The role of prefrontal cortex in action selection, response inhibition, performance monitoring, and reward-based learning,” *Brain Cogn*, vol. 56, no. 2 SPEC. ISS., pp. 129–140, 2004, doi: 10.1016/j.bandc.2004.09.016.

[4] C. D. Chambers, H. Garavan, and M. A. Bellgrove, “Insights into the neural basis of response inhibition from cognitive and clinical neuroscience,” May 2009. doi: 10.1016/j.neubiorev.2008.08.016.

[5] N. J. Kelley, A. Gallucci, P. Riva, L. J. R. Lauro, and B. J. Schmeichel, “Stimulating self-regulation: A review of non-invasive brain stimulation studies of goal-directed behavior,” Jan. 25, 2019, *Frontiers Media S.A.* doi: 10.3389/fnbeh.2018.00337.

[6] A. Bari and T. W. Robbins, “Inhibition and impulsivity: Behavioral and neural basis of response control,” Sep. 2013. doi: 10.1016/j.pneurobio.2013.06.005.

[7] S. F. Logue and T. J. Gould, “The neural and genetic basis of executive function: Attention, cognitive flexibility, and response inhibition,” 2014, *Elsevier Inc.* doi: 10.1016/j.pbb.2013.08.007.

[8] G. Mirabella, “Should I stay or should I go? Conceptual underpinnings of goal-directed actions,” Nov. 03, 2014, *Frontiers Media S.A.* doi: 10.3389/fnsys.2014.00206.

[9] T. Alotaiby, F. E. A. El-Samie, S. A. Alshebeili, and I. Ahmad, “A review of channel selection algorithms for EEG signal processing,” *EURASIP J Adv Signal Process*, vol. 2015, no. 1, Dec. 2015, doi: 10.1186/s13634-015-0251-9.

[10] A. R. Bentivoglio, E. Baldonero, L. Ricciardi, F. De Nigris, and A. Daniele, “Neuropsychological features of patients with Parkinson’s disease and impulse control disorders,” *Neurological Sciences*, vol. 34, no. 7, pp. 1207–1213, Jul. 2013, doi: 10.1007/s10072-012-1224-5.

[11] E. M. Gatto and V. Aldinio, “Impulse Control Disorders in Parkinson’s Disease. A Brief and Comprehensive Review,” *Front Neurol*, vol. 10, Apr. 2019, doi: 10.3389/fneur.2019.00351.

[12] S. Van De Voorde, H. Roeyers, S. Verté, and J. R. Wiersema, “Working memory, response inhibition, and within-subject variability in children with attention-deficit/hyperactivity disorder or reading disorder,” *J Clin Exp Neuropsychol*, vol. 32, no. 4, pp. 366–379, Apr. 2010, doi: 10.1080/13803390903066865.

[13] E. L. Wodka *et al.*, “Evidence that response inhibition is a primary deficit in ADHD,” *J Clin Exp Neuropsychol*, vol. 29, no. 4, pp. 345–356, May 2007, doi: 10.1080/13803390600678046.

[14] R. A. Barkley, “Response inhibition in attention-deficit hyperactivity disorder,” 1999. doi: 10.1002/(SICI)1098-2779(1999)5:3<177::AID-MRDD3>3.0.CO;2-G.

[15] M. Krakowski, “Violence and Serotonin: Influence of Impulse Control, Affect Regulation, and Social Functioning,” 2003.

[16] P. G. Nestor, “Reviews and Overviews Mental Disorder and Violence: Personality Dimensions and Clinical Features,” 2002.

[17] Leah Wright, Jonathan Lipszyc, Annie Dupuis, Sathees Waran Thayapararajah, and Russell Schachar, “Response Inhibition and Psychopathology: A Meta-Analysis of Go/No-Go Task

Performance," *J Abnorm Psychol*, 2014, doi: 10.1037/a0036295.supp.

[18] Pablo Gomez, Roger Ratcliff, and Manuel Perea, "A Model of the Go/No-Go Task," *J Exp Psychol Gen*, 2007, doi: 10.1037/0096-3445.136.3.389.supp.

[19] M. C. Stevens, K. A. Kiehl, G. D. Pearlson, and V. D. Calhoun, "Functional neural networks underlying response inhibition in adolescents and adults," *Behavioural Brain Research*, vol. 181, no. 1, pp. 12–22, Jul. 2007, doi: 10.1016/j.bbr.2007.03.023.

[20] A. R. Aron, "The neural basis of inhibition in cognitive control," Jun. 2007. doi: 10.1177/1073858407299288.

[21] L. Tamm, V. Menon, and A. L. Reiss, "Maturation of Brain Function Associated With Response Inhibition," *J Am Acad Child Adolesc Psychiatry*, vol. 41, pp. 1231–1238, doi: 10.1097/01.CHI.0000020272.43550.5E.

[22] L. Raud, R. Westerhausen, N. Dooley, and R. J. Huster, "Differences in unity: The go/no-go and stop signal tasks rely on different mechanisms," *Neuroimage*, vol. 210, Apr. 2020, doi: 10.1016/j.neuroimage.2020.116582.

[23] A. M. Smith, "AN FMRI INVESTIGATION OF FRONTAL LOBE FUNCTIONING IN PSYCHOPATHY AND SCHIZOPHRENIA DURING A GO/NO GO TASK A THESIS SUBMITTED IN PARTIAL FULFILMENT OF THE REQUIREMENTS FOR THE DEGREE OF DOCTOR OF PHILOSOPHY in THE FACULTY OF GRADUATE STUDIES Program in Neuroscience," 1987.

[24] K. Weidacker, S. Whiteford, F. Boy, and S. J. Johnston, "Response inhibition in the parametric go/no-go task and its relation to impulsivity and subclinical psychopathy," *Quarterly Journal of Experimental Psychology*, vol. 70, no. 3, pp. 473–487, Mar. 2017, doi: 10.1080/17470218.2015.1135350.

[25] T. Parsons and T. Duffield, “Paradigm shift toward digital neuropsychology and high-dimensional neuropsychological assessments: Review,” Dec. 01, 2020, *JMIR Publications Inc.* doi: 10.2196/23777.

[26] Sosa Rodrigo, “Conditioned Inhibition, Inhibitory Learning, Response Inhibition, and Inhibitory Control: Outlining a Conceptual Clarification,” *Psychol Rev*, 2024, doi: 10.1037/rev0000405.supp.

[27] C. P. Panteliadis and C. Author, “Journal of Brain and Neurological Disorders Review Article Historical Overview of Electroencephalography: from Antiquity to the Beginning of the 21 st Century”, doi: 10.5281/zenodo.5359323.

[28] C. A. Tassinari, “An electroencephalographer recalls the history of the Federation on the 70th anniversary of its journal, Clinical Neurophysiology,” Dec. 01, 2019, *Elsevier Ireland Ltd*. doi: 10.1016/j.clinph.2019.10.010.

[29] N. Pradhan and D. Narayana, “A NONLINEAR PERSPECTIVE IN UNDERSTANDING THE NEURODYNAMICS OF EEG,” 1993.

[30] G. Rodríguez-Bermúdez and P. J. García-Laencina, “Analysis of EEG signals using nonlinear dynamics and chaos: A review,” *Applied Mathematics and Information Sciences*, vol. 9, no. 5, pp. 2309–2321, 2015, doi: 10.12785/amis/090512.

[31] N. Schaul, “The fundamental neural mechanisms of electroencephalography,” 1998.

[32] S. Aggarwal and N. Chugh, “Review of Machine Learning Techniques for EEG Based Brain Computer Interface,” Aug. 01, 2022, *Springer Science and Business Media B.V.* doi: 10.1007/s11831-021-09684-6.

[33] G. Li, C. H. Lee, J. J. Jung, Y. C. Youn, and D. Camacho, “Deep learning for EEG data analytics: A survey,” in *Concurrency and Computation: Practice and Experience*, John Wiley and Sons Ltd, Sep.

2020. doi: 10.1002/cpe.5199.

[34] S. Asadzadeh, T. Yousefi Rezaii, S. Beheshti, A. Delpak, and S. Meshgini, “A systematic review of EEG source localization techniques and their applications on diagnosis of brain abnormalities,” Jun. 01, 2020, *Elsevier B.V.* doi: 10.1016/j.jneumeth.2020.108740.

[35] Z. Shou, Z. Li, X. Wang, M. Chen, Y. Bai, and H. Di, “Non-invasive brain intervention techniques used in patients with disorders of consciousness,” 2021, *Taylor and Francis Ltd.* doi: 10.1080/00207454.2020.1744598.

[36] K. Värbu, N. Muhammad, and Y. Muhammad, “Past, Present, and Future of EEG-Based BCI Applications,” May 01, 2022, *MDPI*. doi: 10.3390/s22093331.

[37] Paul L Nunez, “The brain wave equation: a model for the EEG”.

[38] R. Ramele, A. J. Villar, and J. M. Santos, “EEG waveform analysis of p300 ERP with applications to brain computer interfaces,” *Brain Sci*, vol. 8, no. 11, Nov. 2018, doi: 10.3390/brainsci8110199.

[39] A. Khosla, P. Khandnor, and T. Chand, “A comparative analysis of signal processing and classification methods for different applications based on EEG signals,” Apr. 01, 2020, *Elsevier Sp. z o.o.* doi: 10.1016/j.bbe.2020.02.002.

[40] R. E. Dustman, D. E. Shearer, and R. Y. Emmerson, “Life-span changes in EEG spectral amplitude, amplitude variability and mean frequency.”

[41] B. S. Oken, K. H. Chiappa, and B. S. Oken, “Short-term variability in EEG frequency analysis,” 1988.

[42] J. Gotman, “AUTOMATIC RECOGNITION OF EPILEPTIC SEIZURES IN THE EEG,” 1982.

[43] P. Campisi and D. La Rocca, “Brain waves for automatic biometric-based user recognition,” *IEEE Transactions on Information Forensics and Security*, vol. 9, no. 5, pp. 782–800, 2014, doi: 10.1109/TIFS.2014.2308640.

[44] R. W. Thatcher and N. Lab, “COHERENCE, PHASE DIFFERENCES, PHASE SHIFT AND PHASE LOCK IN EEG/ERP ANALYSES.”

[45] A. I. Wang, J. Hokland, and E. A. Larsen, “Master of Science in Computer Science Classification of EEG Signals in a Brain-Computer Interface System,” 2011.

[46] J. S. Kumar and P. Bhuvaneswari, “Analysis of electroencephalography (EEG) signals and its categorization - A study,” in *Procedia Engineering*, Elsevier Ltd, 2012, pp. 2525–2536. doi: 10.1016/j.proeng.2012.06.298.

[47] Borgeat A, Dessibourg C, Popovic V, Meier D, Blanchard M, and Schwander D, “Propofol and spontaneous movements: an EEG study.”.

[48] W. Woaswi, N. Hamzah, W. Omar, A. Saifuddin, W. I. #1, and M. Hanif, “Human Emotion Detection Via Brain Waves Study by Using Electroencephalogram (EEG),” 2018. [Online]. Available: https://www.researchgate.net/publication/329584955

[49] P. Miranda, C. D Cox, M. Alexander, S. Danev, and J. RT Lakey, “Overview of current diagnostic, prognostic, and therapeutic use of EEG and EEG-based markers of cognition, mental, and brain health,” *Integr Mol Med*, vol. 6, no. 5, 2019, doi: 10.15761/imm.1000378.

[50] A. A. Fingelkurts and A. A. Fingelkurts, “Quantitative Electroencephalogram (qEEG) as a Natural and Non-Invasive Window into Living Brain and Mind in the Functional Continuum of Healthy and Pathological Conditions,” Oct. 01, 2022, *MDPI*. doi: 10.3390/app12199560.

[51] D. Brandee and D. Lehmann, “Event-related potentials of the brain and cognitive processes: Approaches and applications,” 1986.

[52] Albert Kok, “Age-related changes in involuntary and voluntary attention as reflected in components of the event-related potential (ERP)”.

[53] J. A. Rushby and R. J. Barry, “Single-trial event-related potentials to significant stimuli,” *International Journal of Psychophysiology*, vol. 74, no. 2, pp. 120–131, Nov. 2009, doi: 10.1016/j.ijpsycho.2009.08.003.

[54] A. S. Al-Fahoum and A. A. Al-Fraihat, “Methods of EEG Signal Features Extraction Using Linear Analysis in Frequency and Time-Frequency Domains,” *ISRN Neurosci*, vol. 2014, pp. 1–7, Feb. 2014, doi: 10.1155/2014/730218.

[55] P. C. Petrantonakis and L. J. Hadjileontiadis, “Adaptive emotional information retrieval from EEG signals in the time-frequency domain,” *IEEE Transactions on Signal Processing*, vol. 60, no. 5, pp. 2604–2616, May 2012, doi: 10.1109/TSP.2012.2187647.

[56] A. Khorshidtalab, M. J. E. Salami, and M. Hamedi, “Robust classification of motor imagery EEG signals using statistical time-domain features,” *Physiol Meas*, vol. 34, no. 11, pp. 1563–1579, 2013, doi: 10.1088/0967-3334/34/11/1563.

[57] Varsha K. Harpale and Vinayak K. Bairagi, *Time and frequency domain analysis of EEG signals for seizure detection: A review*. IEEE, 2016.

[58] W. S. Pritchard and D. W. Duke, “MEASURING CHAOS IN THE BRAIN: A TUTORIAL REVIEW OF NONLINEAR DYNAMICAL EEG ANALYSIS,” 1992.

[59] S. Qian and C. A. Chou, “A Koopman-operator-theoretical approach for anomaly recognition and detection of multi-variate EEG system,” *Biomed Signal Process Control*, vol. 69, Aug. 2021, doi: 10.1016/j.bspc.2021.102911.

[60] W. S. Tirsch, P. Stude, H. Scherb, and M. Keidel, “Temporal order of nonlinear dynamics in human brain,” May 2004. doi: 10.1016/j.brainresrev.2004.01.002.

[61] G. Zamora-López, C. Zhou, and J. Kurths, “Exploring brain function from anatomical connectivity,”

2011. doi: 10.3389/fnins.2011.00083.

[62] S. Noble, D. Scheinost, and R. T. Constable, “A decade of test-retest reliability of functional connectivity: A systematic review and meta-analysis,” *Neuroimage*, vol. 203, Dec. 2019, doi: 10.1016/j.neuroimage.2019.116157.

[63] P. A. Valdes-Sosa, A. Roebroeck, J. Daunizeau, and K. Friston, “Effective connectivity: Influence, causality and biophysical modeling,” Sep. 15, 2011. doi: 10.1016/j.neuroimage.2011.03.058.

[64] P. Babaeeghazvini, L. M. Rueda-Delgado, J. Gooijers, S. P. Swinnen, and A. Daffertshofer, “Brain Structural and Functional Connectivity: A Review of Combined Works of Diffusion Magnetic Resonance Imaging and Electro-Encephalography,” Oct. 07, 2021, *Frontiers Media S.A.* doi: 10.3389/fnhum.2021.721206.

[65] B. He, L. Yang, C. Wilke, and H. Yuan, “Electrophysiological imaging of brain activity and connectivity-challenges and opportunities,” *IEEE Trans Biomed Eng*, vol. 58, no. 7, pp. 1918–1931, Jul. 2011, doi: 10.1109/TBME.2011.2139210.

[66] L. Pessoa, “Understanding brain networks and brain organization,” 2014, *Elsevier*. doi: 10.1016/j.plrev.2014.03.005.

[67] H. E. Wang, C. G. Bénar, P. P. Quilichini, K. J. Friston, V. K. Jirsa, and C. Bernard, “A systematic framework for functional connectivity measures,” *Front Neurosci*, vol. 8, no. DEC, 2014, doi: 10.3389/fnins.2014.00405.

[68] A. M. Bastos and J. M. Schoffelen, “A tutorial review of functional connectivity analysis methods and their interpretational pitfalls,” Jan. 08, 2016, *Frontiers Research Foundation*. doi: 10.3389/fnsys.2015.00175.

[69] L. G. Astrakas and M. I. Argyropoulou, “Shifting from region of interest (ROI) to voxel-based analysis

in human brain mapping," Dec. 2010. doi: 10.1007/s00247-010-1677-8.

[70] S. M. Rajtmajer, A. Roy, R. Albert, P. C. M. Molenaar, and F. G. Hillary, "Avoxelwiseapproachtodetermineconsensusregions-of-interestforthestudyofbrainnetworkplasticity," *Front Neuroanat*, vol. 9, no. JULY, Jul. 2015, doi: 10.3389/fnana.2015.00097.

[71] I. Dinov *et al.*, "Neuroimaging study designs, computational analyses and data provenance using the LONI pipeline," *PLoS One*, vol. 5, no. 9, Sep. 2010, doi: 10.1371/journal.pone.0013070.

[72] E. T. Rolls, C. C. Huang, C. P. Lin, J. Feng, and M. Joliot, "Automated anatomical labelling atlas 3," *Neuroimage*, vol. 206, Feb. 2020, doi: 10.1016/j.neuroimage.2019.116189.

[73] R. A. Heckemann, J. V. Hajnal, P. Aljabar, D. Rueckert, and A. Hammers, "Automatic anatomical brain MRI segmentation combining label propagation and decision fusion," *Neuroimage*, vol. 33, no. 1, pp. 115–126, Oct. 2006, doi: 10.1016/j.neuroimage.2006.05.061.

[74] M. Strotzer, "One century of brain mapping using Brodmann areas," Aug. 2009. doi: 10.1007/s00062-009-9002-3.

[75] J. Huo, J. Wu, J. Cao, and G. Wang, "Supervoxel based method for multi-atlas segmentation of brain MR images," *Neuroimage*, vol. 175, pp. 201–214, Jul. 2018, doi: 10.1016/j.neuroimage.2018.04.001.

[76] D. Ribeiro de Paula *et al.*, "A method for independent component graph analysis of resting-state fMRI," *Brain Behav*, vol. 7, no. 3, Mar. 2017, doi: 10.1002/brb3.626.

[77] R. Srinivasan, P. L. Nunez, and R. B. Silberstein, "Spatial Filtering and Neocortical Dynamics: Estimates of EEG Coherence," 1998.

[78] L. R. Peraza, A. U. R. Asghar, G. Green, and D. M. Halliday, "Volume conduction effects in brain network inference from electroencephalographic recordings using phase lag index," *J Neurosci*

Methods, vol. 207, no. 2, pp. 189–199, Jun. 2012, doi: 10.1016/j.jneumeth.2012.04.007.

[79] U. Malinowska, J. M. Badier, M. Gavaret, F. Bartolomei, P. Chauvel, and C. G. Bénar, “Interictal networks in Magnetoencephalography,” *Hum Brain Mapp*, vol. 35, no. 6, pp. 2789–2805, 2014, doi: 10.1002/hbm.22367.

[80] J. Cao *et al.*, “Brain functional and effective connectivity based on electroencephalography recordings: A review,” Feb. 01, 2022, *John Wiley and Sons Inc*. doi: 10.1002/hbm.25683.

[81] S. Wein *et al.*, “Brain Connectivity Studies on Structure-Function Relationships: A Short Survey with an Emphasis on Machine Learning,” 2021, *Hindawi Limited*. doi: 10.1155/2021/5573740.

[82] J. Luis Perez Velazquez and R. Wennberg, “Coordinated Activity in the Brain Measurements and Relevance to Brain Function and Behavior SPRINGER SERIES IN COMPUTATIONAL NEUROSCIENCE.” [Online]. Available: www.springer.com/series/8164

[83] G. Chiarion, L. Sparacino, Y. Antonacci, L. Faes, and L. Mesin, “Connectivity Analysis in EEG Data: A Tutorial Review of the State of the Art and Emerging Trends,” Mar. 01, 2023, *MDPI*. doi: 10.3390/bioengineering10030372.

[84] S. L. Simpson, F. D. B. Bowman, and P. J. Laurienti, “Analyzing complex functional brain networks: Fusing statistics and network science to understand the brain,” *Stat Surv*, vol. 7, pp. 1–36, 2013, doi: 10.1214/13-SS103.

[85] M. Rubinov and O. Sporns, “Complex network measures of brain connectivity: Uses and interpretations,” *Neuroimage*, vol. 52, no. 3, pp. 1059–1069, Sep. 2010, doi: 10.1016/j.neuroimage.2009.10.003.

[86] S. S. Farley, A. Dawson, S. J. Goring, and J. W. Williams, “Situating ecology as a big-data science: Current advances, challenges, and solutions,” *Bioscience*, vol. 68, no. 8, pp. 563–576, Aug. 2018,

doi: 10.1093/biosci/biy068.

[87] L. Turnbull *et al.*, “Connectivity and complex systems: learning from a multi-disciplinary perspective,” Dec. 01, 2018, *Springer Science and Business Media Deutschland GmbH*. doi: 10.1007/s41109-018-0067-2.

[88] M. Criaud and P. Boulinguez, “Have we been asking the right questions when assessing response inhibition in go/no-go tasks with fMRI? A meta-analysis and critical review,” Jan. 2013. doi: 10.1016/j.neubiorev.2012.11.003.

[89] Y. Tian, S. Liang, and D. Yao, “Attentional orienting and response inhibition: Insights from spatial-temporal neuroimaging,” 2014, *Science Press*. doi: 10.1007/s12264-013-1372-5.

[90] M. Ruchsow *et al.*, “Response inhibition in borderline personality disorder: Event-related potentials in a Go/Nogo task,” *J Neural Transm*, vol. 115, no. 1, pp. 127–133, Jan. 2008, doi: 10.1007/s00702-007-0819-0.

[91] K. A. Kiehl, A. M. Smith, R. D. Hare, and P. F. Liddle, “An Event-Related Potential Investigation of Response Inhibition in Schizophrenia and Psychopathy,” 2000.

[92] D. Asanowicz *et al.*, “The response relevance of visual stimuli modulates the P3 component and the underlying sensorimotor network,” *Sci Rep*, vol. 10, no. 1, Dec. 2020, doi: 10.1038/s41598-020-60268-z.

[93] D. Karamacoska, R. J. Barry, and G. Z. Steiner, “Electrophysiological underpinnings of response variability in the Go/NoGo task,” *International Journal of Psychophysiology*, vol. 134, pp. 159–167, Dec. 2018, doi: 10.1016/j.ijpsycho.2018.09.008.

[94] J. O. Miller, K. Low, G. Logan, J. T. Mordkoff, H. Smid, and R. Ulrich, “Motor Processes in Simple, Go/No-Go, and Choice Reaction Time Tasks: A Psychophysiological Analysis,” 2001.

[95] D. Yon and C. D. Frith, “Precision and the Bayesian brain,” *Current Biology*, vol. 31, pp. R1026–R1032, 2021, doi: 10.1371/currents.tol.

[96] A. Visalli, M. Capizzi, E. Ambrosini, I. Mazzonetto, and A. Vallesi, “Bayesian modeling of temporal expectations in the human brain,” *Neuroimage*, vol. 202, Nov. 2019, doi: 10.1016/j.neuroimage.2019.116097.

[97] S. M. Freeman, S. Itthipuripat, and A. R. Aron, “High working memory load increases intracortical inhibition in primary motor cortex and diminishes the motor affordance effect,” *Journal of Neuroscience*, vol. 36, no. 20, pp. 5544–5555, May 2016, doi: 10.1523/JNEUROSCI.0284-16.2016.

[98] L. Burger, K. Uittenhove, P. Lemaire, and L. Taconnat, “Strategy difficulty effects in young and older adults’ episodic memory are modulated by inter-stimulus intervals and executive control processes,” Apr. 01, 2017, *Elsevier B.V.* doi: 10.1016/j.actpsy.2017.02.003.

[99] D. Struber and J. Polich, “P300 and slow wave from oddball and single-stimulus visual tasks: inter-stimulus interval effects,” 2002.

[100] T. S. Braver and D. M. Barch, “A theory of cognitive control, aging cognition, and neuromodulation.” [Online]. Available: www.elsevier.com/locate/neubiorev

[101] J. M. Bugg and M. J. C. Crump, “In support of a distinction between voluntary and stimulus-driven control: A review of the literature on proportion congruent effects,” *Front Psychol*, vol. 3, no. SEP, 2012, doi: 10.3389/fpsyg.2012.00367.

[102] S. Prezenski, A. Brechmann, S. Wolff, and N. Russwinkel, “A cognitive modeling approach to strategy formation in dynamic decision making,” *Front Psychol*, vol. 8, no. AUG, Aug. 2017, doi: 10.3389/fpsyg.2017.01335.

[103] A. D. Bender, H. L. Filmer, K. G. Garner, C. K. Naughtin, and P. E. Dux, “On the relationship between

response selection and response inhibition: An individual differences approach," *Atten Percept Psychophys*, vol. 78, no. 8, pp. 2420–2432, Nov. 2016, doi: 10.3758/s13414-016-1158-8.

[104] Y. C. Chiu and T. Egner, "Inhibition-induced forgetting results from resource competition between response inhibition and memory encoding processes," *Journal of Neuroscience*, vol. 35, no. 34, pp. 11936–11945, Aug. 2015, doi: 10.1523/JNEUROSCI.0519-15.2015.

[105] J. Kwisthout, H. Bekkering, and I. van Rooij, "To be precise, the details don't matter: On predictive processing, precision, and level of detail of predictions," *Brain Cogn*, vol. 112, pp. 84–91, Mar. 2017, doi: 10.1016/j.bandc.2016.02.008.

[106] W. J. Chai, A. I. Abd Hamid, and J. M. Abdullah, "Working memory from the psychological and neurosciences perspectives: A review," Mar. 27, 2018, *Frontiers Media S.A.* doi: 10.3389/fpsyg.2018.00401.

[107] J. Jonides and D. E. Nee, "Brain mechanisms of proactive interference in working memory," *Neuroscience*, vol. 139, no. 1, pp. 181–193, 2006, doi: 10.1016/j.neuroscience.2005.06.042.

[108] G. Gavazzi *et al.*, "Impulsivity trait and proactive cognitive control: An fMRI study," *European Journal of Neuroscience*, vol. 49, no. 9, pp. 1171–1179, May 2019, doi: 10.1111/ejn.14301.

[109] G. Gavazzi *et al.*, "Subregional prefrontal cortex recruitment as a function of inhibitory demand: an fMRI metanalysis," Sep. 01, 2023, *Elsevier Ltd*. doi: 10.1016/j.neubiorev.2023.105285.

[110] M. Rezvanfard *et al.*, "Evaluation of inhibition response behavior using the Go/No-Go paradigm in normal individuals: Effects of variations in the task design," *Acta Neuropsychologica*, vol. 14, no. 4, pp. 357–366, 2016, doi: 10.5604/17307503.1227530.

[111] H. Meffert, S. Hwang, Z. T. Nolan, G. Chen, and J. R. Blair, "Segregating attention from response control when performing a motor inhibition task. Segregating attention from response control,"

Neuroimage, vol. 126, pp. 27–38, Feb. 2016, doi: 10.1016/j.neuroimage.2015.11.029.

[112] C. H. Cheng, H. Y. Tsai, and H. N. Cheng, “The effect of age on N2 and P3 components: A meta-analysis of Go/Nogo tasks,” *Brain Cogn*, vol. 135, Oct. 2019, doi: 10.1016/j.bandc.2019.05.012.

[113] L. M. Jonkman, M. Lansbergen, and J. E. A. Stauder, “Developmental differences in behavioral and event-related brain responses associated with response preparation and inhibition in a go/nogo task,” in *Psychophysiology*, Society for Psychophysiological Research, 2003, pp. 752–761. doi: 10.1111/1469-8986.00075.

[114] J. L. Smith, S. J. Johnstone, and R. J. Barry, “Movement-related potentials in the Go/NoGo task: The P3 reflects both cognitive and motor inhibition,” *Clinical Neurophysiology*, vol. 119, no. 3, pp. 704–714, Mar. 2008, doi: 10.1016/j.clinph.2007.11.042.

[115] W. Nan, A. P. B. Dias, and A. C. Rosa, “Neurofeedback training for cognitive and motor function rehabilitation in chronic stroke: Two case reports,” *Front Neurol*, vol. 10, no. JUL, 2019, doi: 10.3389/fneur.2019.00800.

[116] T. J. Bosch, C. Groth, T. A. Eldridge, E. Z. Gnimpieba, L. A. Baugh, and A. Singh, “Altered Cerebellar Oscillations in Parkinson’s Disease Patients during Cognitive and Motor Tasks,” *Neuroscience*, vol. 475, pp. 185–196, Nov. 2021, doi: 10.1016/j.neuroscience.2021.08.021.

[117] E. Wascher, S. Arnau, D. Schneider, K. Hoppe, S. Getzmann, and R. Verleger, “No effect of target probability on P3b amplitudes,” *International Journal of Psychophysiology*, vol. 153, pp. 107–115, Jul. 2020, doi: 10.1016/j.ijpsycho.2020.04.023.

[118] N. Benikos, S. J. Johnstone, and S. J. Roodenrys, “Short-term training in the Go/Nogo task: Behavioural and neural changes depend on task demands,” *International Journal of Psychophysiology*, vol. 87, no. 3, pp. 301–312, Mar. 2013, doi: 10.1016/j.ijpsycho.2012.12.001.

[119] J. Albert, S. López-Martín, J. A. Hinojosa, and L. Carretié, “Spatiotemporal characterization of response inhibition,” *Neuroimage*, vol. 76, pp. 272–281, Aug. 2013, doi: 10.1016/j.neuroimage.2013.03.011.

[120] P. D. Gajewski and M. Falkenstein, “Effects of task complexity on ERP components in Go/Nogo tasks,” *International Journal of Psychophysiology*, vol. 87, no. 3, pp. 273–278, Mar. 2013, doi: 10.1016/j.ijpsycho.2012.08.007.

[121] S. A. Los, “The role of response inhibition in temporal preparation: Evidence from a go/no-go task,” *Cognition*, vol. 129, no. 2, pp. 328–344, Nov. 2013, doi: 10.1016/j.cognition.2013.07.013.

[122] M. Moutoussis, P. Fearon, W. El-Deredy, R. J. Dolan, and K. J. Friston, “Bayesian inferences about the self (and others): A review,” 2014, *Academic Press Inc.* doi: 10.1016/j.concog.2014.01.009.

[123] C. Baker, R. Saxe, J. Tenenbaum, and C. L. Baker, “UC Merced Proceedings of the Annual Meeting of the Cognitive Science Society Title Bayesian Theory of Mind: Modeling Joint Belief-Desire Attribution Publication Date Bayesian Theory of Mind: Modeling Joint Belief-Desire Attribution,” no. 33, p. 33.

[124] N. Chater, M. Oaksford, U. Hahn, and E. Heit, “Bayesian models of cognition,” *Wiley Interdiscip Rev Cogn Sci*, vol. 1, no. 6, pp. 811–823, Nov. 2010, doi: 10.1002/wcs.79.

[125] R. van de Schoot *et al.*, “Bayesian statistics and modelling,” Dec. 01, 2021, *Springer Nature*. doi: 10.1038/s43586-020-00001-2.

[126] M. E. Young, S. C. Sutherland, and A. W. McCoy, “Optimal go/no-go ratios to maximize false alarms,” *Behav Res Methods*, vol. 50, no. 3, pp. 1020–1029, Jun. 2018, doi: 10.3758/s13428-017-0923-5.

[127] C. M. Michel and B. He, “EEG source localization,” in *Handbook of Clinical Neurology*, vol. 160, Elsevier B.V., 2019, pp. 85–101. doi: 10.1016/B978-0-444-64032-1.00006-0.

[128] M. A. Jatoi, N. Kamel, A. S. Malik, I. Faye, and T. Begum, “A survey of methods used for source localization using EEG signals,” 2014, *Elsevier Ltd*. doi: 10.1016/j.bspc.2014.01.009.

[129] M. Poncet and J. M. Ales, “Estimating neural activity from visual areas using functionally defined EEG templates,” *Hum Brain Mapp*, vol. 44, no. 5, pp. 1846–1861, Apr. 2023, doi: 10.1002/hbm.26188.

[130] J. Gross, J. Kujala, M. Hä Mä Lä Inen, L. Timmermann, A. Schnitzler, and R. Salmelin, “Dynamic imaging of coherent sources: Studying neural interactions in the human brain,” 2001. [Online]. Available: www.pnas.org

[131] S. P. Van Den Broek, F. Reinders, M. Donderwinkel, and M. J. Peters, “Volume conduction effects in EEG and MEG,” 1998.

[132] J. Holsheimer and B. Feenstra, “VOLUME CONDUCTION AND EEG MEASUREMENTS WITHIN THE BRAIN: A QUANTITATIVE APPROACH TO THE INFLUENCE OF ELECTRICAL SPREAD ON THE LINEAR RELATIONSHIP OF ACTIVITY MEASURED AT DIFFERENT LOCATIONS,” 1977.

[133] F. De Pasquale, S. Della Penna, O. Sporns, G. L. Romani, and M. Corbetta, “A Dynamic Core Network and Global Efficiency in the Resting Human Brain,” *Cerebral Cortex*, vol. 26, no. 10, pp. 4015–4033, Oct. 2016, doi: 10.1093/cercor/bhv185.

[134] S. Achard and E. Bullmore, “Efficiency and cost of economical brain functional networks,” *PLoS Comput Biol*, vol. 3, no. 2, pp. 0174–0183, 2007, doi: 10.1371/journal.pcbi.0030017.

[135] T. Zhou, L. Lü, and Y. C. Zhang, “Predicting missing links via local information,” *European Physical Journal B*, vol. 71, no. 4, pp. 623–630, Oct. 2009, doi: 10.1140/epjb/e2009-00335-8.

[136] R. K. Pan and J. Saramäki, “Path lengths, correlations, and centrality in temporal networks,” *Phys Rev E Stat Nonlin Soft Matter Phys*, vol. 84, no. 1, Jul. 2011, doi: 10.1103/PhysRevE.84.016105.

[137] P. D. Sree Hari, S. K. Prabha, and S. P. Sathian, “The effect of characteristic length on mean free path for confined gases,” *Physica A: Statistical Mechanics and its Applications*, vol. 437, pp. 68–74, Jun. 2015, doi: 10.1016/j.physa.2015.05.022.

[138] Z. Yu *et al.*, “Abnormal topology of brain functional networks in unipolar depression and bipolar disorder using optimal graph thresholding,” *Prog Neuropsychopharmacol Biol Psychiatry*, vol. 96, Jan. 2020, doi: 10.1016/j.pnpbp.2019.109758.

[139] J. Wang, H. Mo, F. Wang, and F. Jin, “Exploring the network structure and nodal centrality of China’s air transport network: A complex network approach,” *J Transp Geogr*, vol. 19, no. 4, pp. 712–721, Jul. 2011, doi: 10.1016/j.jtrangeo.2010.08.012.

[140] V. Gilsing, B. Nooteboom, W. Vanhaverbeke, G. Duysters, and A. van den Oord, “Network embeddedness and the exploration of novel technologies: Technological distance, betweenness centrality and density,” *Res Policy*, vol. 37, no. 10, pp. 1717–1731, Dec. 2008, doi: 10.1016/j.respol.2008.08.010.

[141] B. Luna and J. A. Sweeney, “The emergence of collaborative brain function: fMRI studies of the development of response inhibition,” in *Annals of the New York Academy of Sciences*, New York Academy of Sciences, 2004, pp. 296–309. doi: 10.1196/annals.1308.035.

[142] R. J. Huster, S. Enriquez-Geppert, C. F. Lavallee, M. Falkenstein, and C. S. Herrmann, “Electroencephalography of response inhibition tasks: Functional networks and cognitive contributions,” Mar. 2013. doi: 10.1016/j.ijpsycho.2012.08.001.

[143] L. B. N. Hinkley, S. Vinogradov, A. G. Guggisberg, M. Fisher, A. M. Findlay, and S. S. Nagarajan, “Clinical symptoms and alpha band resting-state functional connectivity imaging in patients with schizophrenia: Implications for novel approaches to treatment,” *Biol Psychiatry*, vol. 70, no. 12, pp.

1134–1142, Dec. 2011, doi: 10.1016/j.biopsych.2011.06.029.

[144] L. Turella, R. Tucciarelli, N. N. Oosterhof, N. Weisz, R. Rumiati, and A. Lingnau, “Beta band modulations underlie action representations for movement planning,” *Neuroimage*, vol. 136, pp. 197–207, Aug. 2016, doi: 10.1016/j.neuroimage.2016.05.027.

[145] Y. Hung, S. L. Gaillard, P. Yarmak, and M. Arsalidou, “Dissociations of cognitive inhibition, response inhibition, and emotional interference: Voxelwise ALE meta-analyses of fMRI studies,” *Hum Brain Mapp*, vol. 39, no. 10, pp. 4065–4082, Oct. 2018, doi: 10.1002/hbm.24232.

[146] M. Sakagami, X. Pan, and B. Uttl, “Behavioral inhibition and prefrontal cortex in decision-making,” *Neural Networks*, vol. 19, no. 8, pp. 1255–1265, Oct. 2006, doi: 10.1016/j.neunet.2006.05.040.

[147] G. Blasi *et al.*, “Brain regions underlying response inhibition and interference monitoring and suppression,” *European Journal of Neuroscience*, vol. 23, no. 6, pp. 1658–1664, Mar. 2006, doi: 10.1111/j.1460-9568.2006.04680.x.

[148] A. Hampshire and A. M. Owen, “Fractionating attentional control using event-related fMRI,” *Cerebral Cortex*, vol. 16, no. 12, pp. 1679–1689, Dec. 2006, doi: 10.1093/cercor/bhj116.

[149] A. L. Lemaitre, G. Herbet, H. Duffau, and G. Lafargue, “Preserved metacognitive ability despite unilateral or bilateral anterior prefrontal resection,” *Brain Cogn*, vol. 120, pp. 48–57, Feb. 2018, doi: 10.1016/j.bandc.2017.10.004.

[150] A. Hampshire and A. M. Owen, “Fractionating attentional control using event-related fMRI,” *Cerebral Cortex*, vol. 16, no. 12, pp. 1679–1689, Dec. 2006, doi: 10.1093/cercor/bhj116.

[151] M. T. Banich, “Executive Function The Search for an Integrated Account,” 2009.

[152] N. Magaia, A. P. Francisco, P. Pereira, and M. Correia, “Betweenness centrality in Delay Tolerant Networks: A survey,” Oct. 01, 2015, *Elsevier B.V.* doi: 10.1016/j.adhoc.2015.05.002.

[153] M. Erika-Florence, R. Leech, and A. Hampshire, “A functional network perspective on response inhibition and attentional control,” *Nat Commun*, vol. 5, Jun. 2014, doi: 10.1038/ncomms5073.

[154] B. J. Levy and A. D. Wagner, “Cognitive control and right ventrolateral prefrontal cortex: Reflexive reorienting, motor inhibition, and action updating,” 2011, *Blackwell Publishing Inc.* doi: 10.1111/j.1749-6632.2011.05958.x.